Title: Inbreeding depression explains killer whale population dynamics

Author list

Marty Kardos[1*†], Yaolei Zhang[2,4*], Kim M. Parsons[1*], Yunga A[2*], Hui Kang[3], Xun Xu[4], Xin Liu[4], Craig O. Matkin[5], Peijun Zhang[3], Eric J. Ward[1], M. Bradley Hanson[1], Candice Emmons[1], Michael J. Ford[1†], Guangyi Fan[2,4,6†], Songhai Li[3, 7†]

Affiliations

[1]Northwest Fisheries Science Center, National Marine Fisheries Service, National Oceanic and Atmospheric Administration; Seattle, WA, USA

[2]BGI-Qingdao, BGI-Shenzhen; Qingdao, 266555, China.

[3]Marine Mammal and Marine Bioacoustics Laboratory, Institute of Deep-sea Science and Engineering, Chinese Academy of Sciences; Sanya, 572000, China.

[4]BGI-Shenzhen; Shenzhen 518083, China.

[5]North Gulf Oceanic Society; Homer, AK, USA.

[6]State Key Laboratory of Agricultural Genomics, BGI-Shenzhen; Shenzhen 518083, China.

[7]Center for Ocean Mega-Science, Chinese Academy of Sciences, Qingdao, 266071, China

* These authors contributed equally.

[†]Address correspondence to:

Marty Kardos (martin.kardos@noaa.gov)

Michael Ford (mike.ford@noaa.gov)

Guangyi Fan (fanguangyi@genomics.cn)

Songhai Li (lish@idsse.ac.cn)

Abstract

Understanding the factors that cause endangered populations to either grow or decline is crucial for preserving biodiversity. Conservation efforts often address extrinsic threats, such as environmental degradation and overexploitation, that can limit the recovery of endangered populations. Genetic factors such as inbreeding depression can also affect population dynamics, but these effects are rarely measured in the wild, and thus often neglected in conservation efforts. Here we show that inbreeding depression strongly influences the population dynamics of an endangered killer whale population, despite genomic signatures of purging of deleterious alleles via natural selection. We find that the 'Southern Residents', which are currently endangered despite nearly 50 years of conservation efforts, exhibit strong inbreeding depression for survival. Our population models suggest that this inbreeding depression limits population growth, and predict further decline if the population remains genetically isolated and typical environmental conditions continue. The Southern Residents also had more inferred homozygous deleterious alleles than three other, growing, populations, further suggesting that inbreeding depression affects population fitness. These results demonstrate that inbreeding depression can substantially limit the recovery of endangered populations. Conservation actions focused only on extrinsic threats may therefore fail to account for key intrinsic genetic factors that also limit population growth.

Main text

Understanding the factors that drive population growth is key to conserving biodiversity. Extrinsic factors, such as habitat loss, climate change, and exploitation by humans, have long been recognized as major drivers of the ongoing decline of natural populations[1-3]. Conservation efforts therefore often focus on addressing extrinsic threats to prevent or reverse population declines. However, depleted populations can be further imperiled by the genetic consequences of small population size, including inbreeding depression (reduced survival or reproduction of the offspring from closely related parents) or the loss of genetic variation and adaptive potential[4-6]. While these genetic factors have long been a theoretical focus in conservation biology[7], intrinsic genetic effects on population dynamics are rarely measured in the wild[8].

A likely genetic threat to depleted populations is inbreeding depression, which is thought to be driven mainly by increased homozygosity for deleterious, partially recessive alleles among inbred individuals[9]. Biologists have long known, mainly from model systems and captive populations, that inbreeding can strongly reduce individual fitness[9-11]. Population models suggest that the levels of inbreeding depression observed in model systems and captivity could decrease the viability of wild populations[5]. Preserving genetic variation and avoiding inbreeding depression have therefore been long standing priorities in conservation biology[7].

The bulk of empirical evidence that inbreeding depression affects population growth in the wild is from genetic rescue studies, where small, inbred populations have nearly universally grown following outbreeding with translocated conspecifics[12]. However, it is usually difficult to determine whether increased population growth following immigration arises from the alleviation of inbreeding depression, the introduction of adaptive alleles, or beneficial environmental changes concurrent with immigration[12,13]. A small number of studies finding positive correlations between population growth and genetic variation in wild populations provide additional evidence for impacts of inbreeding on population dynamics[14,15]. The limited amount, and indirect nature of, empirical evidence for impacts of inbreeding on population viability has led to recent suggestions that there has been too much priority placed on the preservation of genome-wide genetic variation in conservation[16]. Here we address this gap by

directly investigating the impact of inbreeding on the population dynamics of a North Pacific killer whale (*Orcinus orca*) population.

Killer whales in the Eastern North Pacific comprise multiple sympatric ecotypes characterized by differences in diet (mammal-eating 'transients', fish-eating 'residents' and 'offshores'), behavior, and distribution[17-19]. Genetically differentiated populations exist within these ecotypes, and ecotypes differ in patterns of gene flow and dispersal[20]. Population size and trend, extrinsic threats, and conservation status vary among populations, with the 'Southern Resident' killer whale population (SRKW) among the smallest and most threatened.

North Pacific killer whale populations have generally benefitted following legal protections from culls, harassment, and captures for aquaria in the early 1970's[21]. The SRKW is the only major population that has not been generally increasing, although many populations remain vulnerable[22]. The SRKW has remained small (<100 individuals) since the 1970's, and is currently declining and listed as endangered in the United States and Canada, despite nearly 50 years of conservation efforts. The SRKW exhibit low survival and fecundity relative to other populations[23], and are thought to face a number of extrinsic threats, including contaminants, anthropogenic noise and disturbance, and reduced prey abundance[24]. The contrasting population dynamics of the SRKW compared to most other North Pacific populations despite considerable efforts directed at species recovery highlight the need to better understand the factors driving population dynamics.

Results & Discussion

We hypothesized that inbreeding might contribute to fitness variation in killer whales, and may be a factor limiting the growth of the SRKW population compared to other North Pacific killer whale populations. We developed a chromosome-level killer whale reference genome, and sequenced the genomes of 100 SRKWs (77% of the population living after 2002 and ~90% of currently living individuals) and 47 individuals from four other North Pacific populations, including 24 Alaska Residents (ARKW), 2 Northern Residents (NRKW), 14 Transients (TKW), and 7 Offshore individuals (Figure 1A, Extended Data Figure 1).

We first evaluated inbreeding and recent demographic history of each population. We then analyzed the genomes of SRKWs, combined with detailed demographic data from the

population, to estimate inbreeding depression for survival, fecundity, lifetime reproductive success, and population growth. Finally, we compared genomic estimates of inbreeding and the abundance of putatively deleterious alleles and genotypes among populations. The results show that strong survival-mediated inbreeding depression is limiting population growth and recovery of the SRKW.

The SRKW had the highest inbreeding and lowest heterozygosity among the sampled North Pacific killer whale populations. We measured individual inbreeding as the fraction of the genome in runs-of-homozygosity (ROH), which are long homozygous chromosome segments caused by common ancestors of parents (F_{ROH}). We measured F_{ROH} using minimum ROH lengths of 1Mb ($F_{ROH,1Mb}$), and 10Mb ($F_{ROH,10Mb}$) because the abundance of ROH of different lengths may differentially affect fitness[25-27]. For example, the longest ROH ≥10Mb have more recent average coalescent times than shorter ROH[28] and are therefore often enriched for deleterious alleles that have been exposed to selection for a short time[29,30]. Shorter ROH arise from coalescent events in deeper history, and can therefore be informative of deep historical demographic events (e.g., population bottlenecks and founder events[31]). Average F_{ROH} was highest in the SRKW population (Figures 1B, 1C), where $F_{ROH,1Mb}$ ranged from 0.18 to 0.44. Twelve of the SRKWs had $F_{ROH,10Mb} > 0.0625$, the inbreeding expected for the offspring of first cousins. The resident ecotype populations had the lowest average genome-wide heterozygosity (H, the average fraction of the genome in heterozygous SNPs) among the three sampled ecotypes (Supplementary Table 16). The SRKW had the lowest ($H = 0.00029$), and the TKW had the highest heterozygosity ($H = 0.00058$) across the sample populations. The elevated inbreeding and lower H in the SRKW are consistent with a history of smaller effective population size (N_e), and/or greater reproductive isolation in the SRKW[32-34] compared to other populations.

Linkage disequilibrium (LD) based estimates of recent N_e[35,36] for the SRKW, ARKW, and TKW (the three populations with the largest sample sizes), suggest that all three populations have contemporary $N_e < 100$ (Figure 1E; $N_e = 27.4$ [SRKW], $N_e = 38.9$ [ARKW], and $N_e = 86$ [TKW]) and that N_e in each population declined substantially ~25-30 generations ago (~625-750 years, assuming 25-year generations[23]) (Figure 1D). The SRKW had a relatively small and consistent N_e (ranging from $N_e = 61$ to $N_e = 76$) over the most recent ~30 generations (Figure 1D, Extended Data Figure 2). Estimated N_e prior to ~30 generations ago was substantially larger for TKW ($N_e \geq 3{,}000$) than for either SRKW or ARKW ($N_e < 750$) (Figure 1D). Previous

coalescent-based analyses of deep demographic history[31] suggested that N_e was ≈ 5,500-6,000 between 10,000 and 100,000 thousand years (~400-4,000 generations) ago for transient killer whales. The same analysis[31] suggested that, after an expansion from N_e ≈ 5,000 to N_e ≈ 6,500 between 100,000 and 40,000 years ago, the ancestral population(s) of resident killer whales declined to N_e ≈ 600 by 10,000 years (~400 generations) ago. Therefore, the ancestral population(s) of both ARKW and SRKW appear to have been relatively small both recently (up to 150 generations ago), and in deeper population history (~10,000 years ago). Inferred patterns of historical N_e based on LD can be influenced by both changes in population size and gene flow[35,37]. The relative contribution of changes in population-specific N_e versus changes in gene flow to estimates of N_e is unclear in this case, but the very large historical N_e of the TKW (> 3,000) is likely due to more extensive historical connectivity with other killer whale populations compared to the SRKW and ARKW.

The analysis of effective population size suggests that the elevated inbreeding and lower H in the SRKW is likely due to small local N_e (Figures 1D, 1E) combined with a lack of recent incoming gene flow. No SRKW progeny from extra-population mating events have been detected through parentage analysis over the last 1-2 generations[33] (Supplementary Table 6), and immigration from other North Pacific resident populations has not been observed over the nearly 50 years of field studies[34]. However, the still relatively low inbreeding in the SRKW (Figures 1B, 1C) compared to some long-isolated, or extremely bottlenecked small populations[38-42], and low genetic differentiation among resident population(s) (Supplementary Figure 5)[43] suggest that the genetic isolation of the SRKW is relatively recent in terms of number of generations. H is expected to decline at a rate of $1/2N_e$ per generation in a closed population. The reduction of H in the SRKW relative to an ancestral population assumed to have the same H as the ARKW (Supplementary Table 16) would therefore require 20 generations (~500 years) of complete isolation, assuming the inferred historical SRKW N_e shown in Figure 1D (Supplementary Methods). We interpret this estimate of 20 generations as the minimum divergence time of the SRKW from other populations under the assumption of complete isolation. The rather small estimated N_e for the SRKW over the last ~30 generations (Figure 1D, Extended Data Figure 2) could therefore be related to a temporal change in gene flow during this time frame.

We tested whether survival and fecundity in the SRKW population were related to F_{ROH}. Using Bayesian logistic regression models, we found that survival rates declined substantially

with increasing F_{ROH} in the SRKW population (Figure 2A, Extended Data Figures 3-7; Table 1), while controlling for effects of age, sex, and yearly environmental variation[23]. The posterior distribution for the F_{ROH} effect on annual survival in this model ($B_{F_{ROH}}$) was strongly negative for both ROH length-based definitions of F_{ROH} (Table 1, Supplementary Tables 9-11). Annual survival probability for an average 20 year-old killer whale declined by >3% (from 0.994 to 0.960) for females and by nearly 5% (from 0.990 to 0.942) for males with the highest observed inbreeding in the population ($F_{ROH,10Mb} = 0.14$) compared to $F_{ROH,10Mb} = 0$ (Extended Data Figure 3). More highly inbred individuals also died substantially younger than those with the smallest values of $F_{ROH,10Mb}$ (Extended Data Figure 7). The cumulative probability of surviving to 40 years (i.e., through the reproductive years for females) declined by 64% (from 0.84 to 0.30) for females and by 78% (from 0.76 to 0.17) for males with $F_{ROH,10Mb} = 0.14$ compared to $F_{ROH,10Mb} = 0$ (Extended Data Figure 4). Survival over the long term is a crucial fitness component in killer whales, where female age at first reproduction is >10 years, and average fecundity is highest among females in their early 20s (Supplementary Figure 13)[23]. The effect of $F_{ROH,10Mb}$ on survival resulted in a 41% decline (from 2.53 to 1.49) in expected lifetime reproductive success among the most highly inbred females (Extended Data Figure 8). In addition to F_{ROH}, we used the heterozygous proportion of all SNPs in the genome (H_{SNP}) as an alternative genomic measure of inbreeding in the survival analysis[8]. The effects of $F_{ROH,1Mb}$ and H_{SNP} on survival were nearly identical to that of $F_{ROH,10Mb}$ (Table 1, Extended Data Figures 3-6). Sex-specific estimates of haploid lethal equivalents[44] for annual survival were $b = 0.10$ for females and $b = 0.14$ for males. There were $b = 3.74$ lethal equivalents for males and $b = 2.74$ for females with respect to survival to 40 years.

These analyses likely underestimated the effects of inbreeding on mortality because we have no data on these effects in the earliest life stages (before or shortly after birth) when inbreeding depression is often strongest[45] and when highly deleterious alleles are likely to act[46-48]. The inbreeding depression we detect here is therefore likely driven by the polygenic component of the inbreeding load. The potential additional contribution of large-effect deleterious alleles to early life survival[46-48] is unclear. There was no evidence for an effect of inbreeding on annual fecundity (Supplementary Tables 12-13). However, we likely had lower power to detect inbreeding depression for fecundity than for survival because many pregnancies and some births go unobserved in our study system[49].

We ran two sets of individual-based simulations parameterized using demographic data from the last nearly 50 years to evaluate the effect of inbreeding depression on SRKW population dynamics. The first set of simulations incorporate genetically explicit models of the inbreeding depression we detected in the SRKW. In these models, inbreeding depression for survival is driven by simulated deleterious mutations to allow *b* to change through time as expected with purifying selection and genetic drift[50]. The inbreeding load (*b*) at the beginning of the simulations of future population dynamics was closely matched to that estimated for the real population as described above. To determine whether population growth would be higher in the absence of this inbreeding depression, we ran a second set of simulations where the age- and sex-specific survival probabilities associated with the least inbred (highest heterozygosity) SRKWs (Figure 2A, Extended Data Figures 3-6) were applied to all individuals. Note than the least inbred SRKW have inbreeding typical of the ARKW (Figures 1B-C, 3B), a population of the same ecotype that has grown substantially since protection in the 1970s[51]. If inbreeding depression limits SRKW population growth, the projected future population sizes should be smaller under the first set of simulations where inbreeding depression is included than in the second set of simulations where it is not.

The simulations that include inbreeding depression project declining population size over the next 100 years (Figure 2B) under a wide range of assumptions regarding the genetic basis of inbreeding depression (distribution of fitness effects and dominance of deleterious alleles, Supplementary Table 15, Extended Data Figure 9). The simulations without inbreeding depression project increasing population size through time (Figure 2B, Extended Data Figure 9). All of these simulations were conducted under an assumption of a constant environment typical of the average of the last 40 years. They are therefore intended to explore the effects of inbreeding depression on population dynamics, and will not necessarily be an accurate prediction of future population growth under different environmental conditions. While environmental factors or disturbances have clearly influenced population dynamics of the SRKW[23,24,52-54], our results suggest that inbreeding depression has also been an important factor limiting the growth and recovery of the population since protections in the 1970s.

To further explore possible effects of inbreeding on fitness, we used molecular[55] and population genetic[56] analyses to evaluate the relative genetic loads and possible fitness effects of inbreeding among North Pacific populations. We identified >28,000 putatively deleterious alleles

as derived alleles arising from missense or loss-of-function [LOF] mutations (Supplementary Figures 14-15), and then compared their abundance across the three populations with the largest sample sizes: the SRKW, ARKW, TKW. LOF alleles were less frequent in the SRKW than in the ARKW population (Figure 3A), suggesting that selective purging of strongly deleterious alleles has removed some highly deleterious alleles in the SRKW compared to the ecologically similar but larger ARKW population. However, LOF alleles were more abundant in both SRKW and ARKW than in the TKW population, likely due to stronger genetic drift associated with the smaller long-term historical N_e of the SRKW and ARKW (Figures 1D, 3A)[31]. The abundance of missense mutations, which are expected to have smaller effects than LOF mutations, was similar across these three populations (Figure 3A). The site frequency spectra showed that putatively deleterious alleles had lower average frequencies than putatively neutral alleles within each population (Extended Data Figure 10) ($P < 0.0001$, randomization tests), suggesting that natural selection has purged part of the genetic load in each population, and that our measure of genetic load was informative of historical fitness.

However, deleterious alleles are generally at least partially recessive[9], so the deleterious genetic effects on fitness are likely determined more by the number of homozygous deleterious genotypes (the homozygous mutation load) than the allele frequencies. The homozygous mutation load was highest in the SRKW (average number of homozygous deleterious alleles >4,000), and approximately half of this load was due to fixed alleles (Figures 3B, 3C). The lower average homozygous mutation load in the other populations appeared to be primarily due to fewer fixed putatively deleterious alleles (Figure 3C). For example, <500 putatively deleterious alleles were fixed in the TKW population, accounting for less than 1/6 of the total number of homozygous deleterious alleles in that population (Figure 3C). Variation in the abundance of fixed putatively deleterious alleles among populations may also explain why individuals with similar F_{ROH} (e.g., $F_{ROH,1Mb} \approx 0.15$ in Figure 3B) sampled from different ecotypes often had substantially different homozygous mutation loads. The variation among populations in the homozygous mutation load (and by extension fitness) therefore appears to be determined not only by differences in inbreeding among populations (as observed elsewhere[57]), but also by the historical population processes of genetic drift, selection, and gene flow that drove the loss or fixation of deleterious alleles in our study system both recently (Figure 1D) and in deep population history[31]. This result suggests that historical fixation of putatively deleterious alleles

(the demographic impact of which can only be alleviated by immigration), and relatively high inbreeding contribute to the lower average fitness in the SRKW compared to the other populations. This is consistent with the observed mortality-mediated inbreeding depression in the SRKW (Figure 2, Extended Data Figures 3-7) and the higher population growth rates of the other North Pacific populations compared to the SRKW[24,51,58,59].

Conclusions and conservation implications

The evolutionary importance of inbreeding depression has been apparent since Darwin's experiments with plants in the 19th century[9]. Subsequent empirical evidence for inbreeding depression, mainly from model and agricultural study systems, together with predictions arising from theoretical population genetics, have made inbreeding depression and the preservation of genetic variation central concerns in conservation biology[4,7]. Despite this focus, there have been few direct empirical measurements of the effects of inbreeding depression on the population dynamics of wild populations, meaning that one of the central tenets of conservation biology is still largely based on theoretical expectations and results in model systems, captive populations, and agriculture. Our results help to fill this gap by providing direct evidence that deleterious genetic variation and inbreeding depression for survival substantially impact population dynamics in an endangered population.

These results are relevant to our understanding of the influence of historical population size and natural selection on contemporary inbreeding depression. Several recent genomics studies found evidence of purging of large-effect deleterious alleles in small wild populations[38,40,57,60-64]. Some have suggested that long-term small historical N_e and genomic evidence for purging imply that inbreeding depression is likely to be weak[38,61,63]. The results from our demographic analysis demonstrate that inbreeding depression can be strong despite the purging of deleterious alleles (Figure 3A, Extended Data Figure 10) associated with long-term small historical N_e (Figure 1D)[31,50,65]. In this way, our results are similar to those in Soay sheep, which also show substantial inbreeding depression for survival ($b \approx 2.3$)[45], despite having resided in the Outer Hebrides with small population size (contemporary $N_e < 200$)[66] for thousands of years[67]. This underscores the importance of detailed demographic analyses to understand inbreeding depression[45,68,69], and that historically small N_e and partial purging of deleterious

307 variation does not imply that inbreeding depression is weak or unlikely to substantially affect
308 population dynamics.
309 To date, conservation efforts for North Pacific killer whales, and marine mammals more
310 broadly[70,71], have largely, and often successfully, focused on mitigating extrinsic environmental
311 threats. Protection from direct harm (capture and intentional killing), and continuing efforts to
312 address extrinsic threats such as prey abundance[72], toxic pollution[24], and vessel traffic[52-54], have
313 contributed to sustained population growth of many (but not all[73]) North Pacific killer whale
314 populations since the 1970s[51,58]. While these efforts have also reduced environmental threats to
315 the SRKW, they have not resulted in the sustained population growth observed in many other
316 North Pacific populations[59]. Continuing to address ongoing environmental threats to the SRKW
317 and other populations is unquestionably important, but our results show that inbreeding
318 depression is also important in limiting the recovery of the SRKW population. In fact, our results
319 suggest that the SRKW population growth rate would be substantially higher if its average level
320 of inbreeding was similar to other North Pacific killer whale populations.
321 A combination of natural and anthropogenic extrinsic factors likely led to the small
322 population size, elevated inbreeding, and low fitness of the SRKW compared to other North
323 Pacific populations. First, the SRKW are on the southern edge of the geographic range of North
324 Pacific resident ecotype, which may have contributed to its historically smaller size and lack of
325 reproductive connectivity to other populations[74,75]. Second, the SRKW population was much
326 more heavily impacted by live captures during the 1960s-1970s than other populations, resulting
327 in the removal of about 50 individuals in addition to accidental deaths[21]. The differential impact
328 of the live captures certainly reduced population size and may have contributed to the increased
329 inbreeding in the SRKW compared to other populations. Finally, the SRKW share salmon prey
330 resources with other North Pacific killer whale populations, and populations of other rapidly
331 recovering marine mammals[76,77]. The higher inbreeding in the SRKW compared to these other
332 populations may have put the SRKW at a competitive disadvantage as overall killer whale
333 abundance increased after 1970 and prey became a more limiting resource[78]. Extrinsic threats
334 (either natural or anthropogenic) therefore appear to have created the conditions (isolation, small
335 size) for inbreeding depression to further threaten population viability. This highlights the
336 importance of addressing extrinsic threats before they lead to conditions where inbreeding
337 depression becomes a significant limiting factor[3,6]. This conclusion is reinforced by the

demographic collapse of a small, inbred Atlantic killer whale population that was also hypothesized to be exacerbated by inbreeding depression[31,79].

The importance of inbreeding to population growth suggests that in addition to mitigating extrinsic environmental threats, addressing genetic risks, if possible, would also benefit the SRKW population. Genetic rescue through introduction of unrelated individuals has been a successful conservation strategy for numerous wild populations suffering from inbreeding depression[12]. However, genetic rescue through translocation would be both logistically challenging and unlikely to elicit gene flow in the case of the SRKW population. The population's geographic range already overlaps with multiple other killer whale populations (Figure 1A). The population is therefore reproductively isolated by behavior rather than by geographic barriers to gene flow. The relatively low genetic differentiation and proximity of the SRKW to other populations[43] (Supplementary Figure 5) suggests that occasional natural interbreeding might be a realistic scenario that could alleviate inbreeding depression, but such interbreeding has not been observed. A plausible interpretation of the historical N_e estimates and the current levels of heterozygosity is that the SRKW population was more connected to other populations as recently as ~30 generations ago (Figure 1D). Sporadic gene flow events may therefore be a natural part of the life history of this species, and if such events were to occur, the SRKW population would likely grow due to reduced inbreeding. If, on the other hand, the SRKW population remains both genetically isolated and small, inbreeding depression will likely become an even greater threat to the population's persistence in the future as inbreeding increases through time.

Methods

Population history

The SRKW population has fluctuated in abundance between 67 and 98 animals over the past ~48 years, and as of 2020 had a population size of 72, compared to 71 in 1974[80]. The ARKW is part of a larger Alaskan metapopulation; the whales included here represent a population of >700, and is estimated to have more than doubled in abundance between 1984 and 2010[58,76]. The NRKW population size was ~302 in 2018, increasing from ~122 in 1974[81]. The Offshore

population is estimated at >300, with an unknown trend, and the TKW is estimated at >243 with rapid growth from the 1970's to 1990s and an unknown recent trend[80].

Sample Collection and Sequencing

For the genome assembly, a blood sample from a male killer whale was collected on 30 March, 2019 in captivity, under an Ethical Statement of the Institute of Deep-sea Science and Engineering, Chinese Academy of Sciences (IDSSE-SYLL-MMMBL-01). The sampled whale was originally from the Northwest Pacific Ocean and estimated to be around 10 years old during sampling. DNA was isolated from this sample using cetyl trimethylammonium bromide (CTAB)[82] for a new reference genome sequence and assembly. Demographic information for the SRKW population was obtained from long-term field studies[83,84]. Tissue samples for resequencing were collected as previously described[33], under National Marine Fisheries Service General Authorization No. 781–1725, and scientific research permits 781-1824-01, 16163, 532-1822-00, 532– 1822, 10045, 18786-03, 545-1488, 545-1761, and 15616. DNA was isolated from 151 skin samples using Qiagen DNeasy® Blood and Tissue kits, or phenol-chloroform-isoamyl alcohol genomic DNA extraction methods[85]. For the reference genome assembly, one Oxford Nanopore Technology (ONT) library and one HI-C library were constructed following the manufacturer's protocols. The ONT library was sequenced using the GridION X5 platform. For resequencing, libraries with an average insert size of ~350 bp were generated for the 151 DNA samples and the DNA isolated from the blood sample (for error correction during genome assembly) according to the MGIEasy FS DNA Library Prep Set kit (MGI, China). Whole genome sequencing libraries and Hi-C library were sequenced using the BGISEQ-500 platform, yielding paired-end reads with a length of 100 bp.

Killer Whale Genome Assembly and annotation

For the genome assembly, NextDenovo (v2.1, https://github.com/Nextomics/NextDenovo) was firstly used to assemble the initial contigs based on ~399.38 Gb Nanopore long reads (Supplementary Table 1). Subsequently, Soapnuke (v1.6.5)[86] was used to perform data filtering with parameters "-l 10 -q 0.1 -n 0.05 -Q 2 -d" for the ~152.66 Gb short paired-end data, which was then used to polish the initial contigs by running two-rounds of Pilon (v1.23)[87] pipeline. Finally, the polished contigs were anchored to chromosomes by utilizing HiC-Pro pipeline[88] with parameters "[BOWTIE2_GLOBAL_OPTIONS = --very-sensitive -L 30 --score-min L,-0.6,-0.2 -

-end-to-end –reorder; BOWTIE2_LOCAL_OPTIONS = --very-sensitive -L 20 --score-min L,-0.6,-0.2 --end-to-end –reorder; IGATION_SITE = GATC; MIN_FRAG_SIZE = 100; MAX_FRAG_SIZE = 100000; MIN_INSERT_SIZE = 50; MAX_INSERT_SIZE = 1500]" (Supplementary Figures 1-2) and 3D-DNA pipeline[89] with parameters "-m haploid -s 0 -c 22" using ~135.90 Gb Hi-C data, generating a 2.35 Gb genome assembly with contig N50 of 34.75 Mb. And 99.03% of the contig sequences could be anchored into 22 chromosomes with lengths ranging from 35.29 to 183.77 Mb (Supplementary Table 1-3, Supplementary Figure 3). This reference genome is a substantial improvement over the previously available draft genome[90], increasing the contig N50 494.55-fold and decreasing the gap length 971.16-fold (Supplementary Table 2). We then used homology-based and *de novo* predictions of protein-coding genes to annotate the genome (Supplementary Methods).

Variant Calling

We generated ~6.92 Tb of sequence data with an average sequencing depth of ~19.45 per sample (Supplementary Table 5). Raw sequencing data for the 151 samples were filtered using Soapnuke (v1.6.5)[86] to remove low quality, adapter contaminated and PCR duplicated reads. Next, filtered clean reads were aligned to our chromosome-level killer whale reference genome using the BWA (v0.7.12-r1039)[91] with default parameters. SAMtools (v0.1.19-44428cd)[92] was used to convert SAM files to BAM format and to sort alignments, followed by Picard package (v1.54), which was used to remove duplicates and GATK (v3.8-1-0)[93], which was used to re-align the reads around InDels. SNP calling was also carried out using GATK (v3.8-1-0)[93] with the joint calling method. In detail, we got the genomic variant call format (GVCF) in ERC mode based on read mapping with parameters "-T HaplotypeCaller, -ERC GVCF, -variant_index_type LINEAR, -variant_index_parameter 128000, and -mq 20"), and then conducted joint variant calling with module "CombineGVCFs" in GATK. Finally, module "VariantFiltration" in GATK was used to carry out hard filter with parameters "—filterExpression QD < 2.0 || MQ < 40.0 || FS > 60.0 || ReadPosRankSum < -8.0 || MQRankSum < -12.5 || SOR >3.0". Four of the 151 original samples were excluded from downstream analyses after quality control checks (Supplementary Methods, Supplementary Table 5). We identified the sex chromosome as chromosome 6 in our genome assembly (Supplementary Table 3)

Genomic Analysis of Inbreeding

To evaluate ROH, we first filtered the SNPs in VCF format to remove loci likely to decrease the accuracy of the identified ROH. We removed loci that had a minor allele frequency < 0.05 in order to remove loci that are more likely to have arisen from sequencing or read mapping errors. In order to further remove loci with poor read mapping (e.g., in duplicated genomic regions which are common in mammalian genomes) we removed any locus that had a *P*-value <0.01 for an exact test for an excess of heterozygotes relative to Hardy-Weinberg proportions across all populations, or had mean SNP read depth <5 or >17[27,41] (Supplementary Figure 16). To detect ROH, we used a likelihood-based approach that accounts for variation in allele frequencies and for sequencing errors[27,41,57,94]. As in Khan et al.[57], we modified this approach to use genotype likelihoods as input rather than called SNPs in order to take full advantage of genomic information contained in all sequence reads, including sites with too few reads to reliably call individual genotypes.

Effective Population Size

We used the LD-based method implemented in GONE[35] to estimate a time series of recent N_e for SRKW, ARKW, and TKW. GONE uses patterns of LD among loosely linked SNPs to estimate N_e a few generations ago, and LD between closely linked SNPs (where intervening recombination events are rare) to estimate deeper historical N_e. We used called autosomal SNP genotypes after filtering out genotypes with GQ<20, removing individuals missing genotypes at >10% of SNPs, and requiring a minimum minor allele count of 2 within each population. This resulted in sample sizes of 75 (SRKW), 19 (ARKW), and 13 (TKW) for the analysis in GONE. We assumed a constant recombination rate of 1 cM/Mb (a typical recombination rate among large mammals). We included a maximum of 10,000 SNPs per chromosome in the analysis and applied Haldane's correction for genetic distance[35]. The analysis was carried out only on pairs of loci within 2 cM (default = 5 cM) according to the assumption of 1 cM/Mb (parameter *hc* was set to 0.02) to mitigate the possibility of bias arising from population substructure in recent population history[35]. The analysis was repeated 500 times, each time with a different randomly selected set of 10,000 SNPs/chromosome; these analysis repetitions were used to calculate the confidence intervals for historical N_e in Figure 1C. We estimated contemporary N_e based on the LD among unlinked SNPs using NEESTIMATOR (v. 2.1)[36] using the same data as with GONE.

The LD-based estimates of N_e from patterns of LD among unlinked SNPs in NEESTIMATOR are informative of N_e in the parental generation of the sampled individuals[36].

Genetic Load

We used our genome annotations, and the Ensembl Variant Effect Predictor (VEP, release 103)[55] to identify alleles that are likely to negatively affect fitness. We identified the ancestral allele at each SNP identified in killer whales as the majority allele among Pacific white-sided dolphin (*Lagenorhynchus obliquidens*), Atlantic right whale (*Eubalaena glacialis*), and Indo-Pacific dolphin (*Tursiops aduncus*) reference genome sequences. The reference genomes were obtained as follows: Indo-Pacific dolphin (https://www.ncbi.nlm.nih.gov/assembly/GCA_003227395.1), North Atlantic right whale (https://www.dnazoo.org/assemblies/Eubalaena_glacialis), Pacific white-sided dolphin (https://www.dnazoo.org/assemblies/Lagenorhynchus_obliquidens) on 20 October, 2020. We used the getFasta command in bedtools[95] to generate a FASTA file made of short (70 bp) sub-sequences covering the entirety of each of these three reference genomes. For each chromosome, we extracted 70 bp fragments with fragment starting points separated by 10 bp (i.e., adjacent fragments were tiled such that they overlapped by 60 bp) to increase the proportion of sites successfully mapped to the killer whale reference genome. We converted these FASTA files to FASTQ format and then aligned the sequence data to our new killer whale reference genome using BWA (v. 0.7.17) mem[91]. We converted the aligned reads from SAM to BAM format and then sorted the BAM files using SAMtools (v. 1.11) view[96]. We used the SAMtools mpileup command to generate a BCF file containing the alleles present at each killer whale SNP position. We then used BCFtools (v. 1.11)[96] to convert the BCF file to VCF format. We used the resulting VCF to identify the ancestral allele as the majority allele among the three species' reference genomes. Loci missing data for one or more species were not polarized, and thus excluded from the analysis. We identified deleterious alleles as derived alleles at loci where the VEP identified missense (likely moderately deleterious) or loss-of-function (likely highly deleterious) variants. We estimated individual homozygous mutation load (Figure 3, Supplementary Figures 10, 11) as the number of homozygous derived alleles at loci identified by VEP as carrying putatively highly or moderately deleterious mutations.

We also compared effects of purifying selection among populations using the $R_{X/Y}$ approach of Do et al.[56]. Following Do et al.[56], we calculated $R_{X/Y}$ as the expectation for the number of derived alleles present in a randomly selected haploid genome from population X that are not present in randomly selected haploid genome population Y. We measured the sampling error of $R_{X/Y}$ (i.e., the error bars in Figure 3A) as the standard deviation among estimates of $R_{X/Y}$ derived from 100 rounds of resampling the data using a block jackknife approach (with 100 blocks equal size blocks)[56,60]. We conducted the $R_{X/Y}$ analysis after equalizing the number of genomes per population to 12 diploid individuals. The genetic load analyses are based on the same individuals and filtered SNPs as in the genomic analysis of inbreeding described above, except here we did not require a minimum minor allele frequency. Methods used to estimate the site frequency spectrum are in the Supplementary Methods.

Inbreeding depression in the Southern Resident killer whales

Survival model – We constructed an age-based survival model, using census data after 1976[84], and animals born after 1960 to avoid uncertainty and biases associated with older ages early in the field study[23] (Supplementary Table 8), which resulted in a sample size of 85 animals (2,169 animal-year observations). Because of unknown ages of some animals at the start of the time series, previous modelling efforts have used stage-based survival models[33] – but by not including animals with unknown ages we were able to fit a more specific model using ages rather than stages[23,97]. The base model is

$$logit(\phi_{a,y}) = B_{0,sex} + s(year, k = 7) + s(age, k = 5) + B_{F_{ROH}} * F_{ROH_a}, \qquad \text{eq. 1}$$

where $\phi_{a,y}$ is the probability of survival of animal a in year y, $B_{0,sex}$ is a sex-specific intercept, and $B_{F_{ROH}}$ is an estimated coefficient relating the F_{ROH_a} value for animal a to survival. The s() functions represent penalized regression smooths on effects of age and year; these functions include knots specified to represent the complexity or wiggliness of the function. The age effect is flexible to capture the U-shaped mortality observed in long lived species including killer whales[18], and the year effect is included to capture broader environmental variation, (attributed to changes in prey or other factors) that influences variation in demographic rates. We assumed the effect of F_{ROH} was linear in logit-space, and estimated it with the coefficient $B_{F_{ROH}}$. We assigned standard normal priors to all fixed effects, and Student-t priors to variance parameters.

We conducted two sensitivity analyses with this general approach. First, to ensure the robustness of our results for the survival models, we re-fit the 1-stage survival in a maximum likelihood framework, using generalized additive models in the `mgcv` package in R; like in the Bayesian analysis, the estimated F_{ROH} coefficients were negative and statistically significant (Supplementary Table 9). Second, we took a similar approach to Ford et al.[33], and constructed a 2-stage Bayesian model that involved first fitting an initial model to animals that don't have genetic data (76 animals), and using the posterior from those fixed effects as a prior for a second model, fit to animals with genetic data (85 animals with known ages; Supplementary Table 10). Second, we examined the sensitivity to the choice of priors on fixed effects, replacing standard normal priors with improper (flat) ones using the `brms` R package[98] (Supplementary Table 11). Each of these alternative analysis approaches yielded similar results to those reported above.

Fecundity model – We adopted a similar approach with an age–based model with fecundity data. Because of uncertainty and bias in female ages in the 1970s[23,84], animals born before 1960 were not included, which resulted in a sample size of 42 females. The initial base model constructed was of the form

$$logit(\theta_{a,y}) = B_0 + B_1 * age + B_2 * age^2 + s(year, k = 7) + B_{F_{ROH}} * F_{ROH_a}, \quad \text{eq. 2}$$

where $\theta_{a,y}$ represents the probability of giving birth. Like the survival model, the $s()$ function represents an estimated smooth function to capture broader environmental variation, and the remaining fixed effect coefficients allow for a quadratic effect of age (output in Supplementary Table 12). Like with survival, we assumed a linear effect of F_{ROH} in logit-space. Also, like the survival model, we repeated the fecundity analysis using 2-stage Bayesian model (output summarized in Supplementary Table 13).

Estimation – Bayesian Estimation for all models was performed using R (v4.1.2) (R Core Development Team 2021) and using Stan via the brms[98] and cmdstanr packages[99]. Stan implements Markov chain Monte Carlo (MCMC) using the No-U Turn Sampling (NUTS) algorithm[100,101]. Each model was run with 4 parallel MCMC chains, for 5,000 iterations (5,000 warmup). Convergence was assessed by monitoring the lack of divergent transitions, trace plots, and R-hat statistics[102].

549 *Effect sizes* – Because of negative relationships between F_{ROH} and survival rates, we
550 calculated the effects of both of the ROH length-based definitions of F_{ROH} ($F_{ROH,1Mb}$, $F_{ROH,10Mb}$)
551 on annual survival probability across the range of F_{ROH} values observed in our dataset. Using
552 output from our Bayesian models, we generated estimates of the predicted male and female killer
553 whale survival rates for a reference year (2000) and age (20) across all values of F_{ROH}; other
554 years or ages could be used, and shift the intercept up or down (but don't influence the trend). As
555 these annual survival probabilities are generally very high (even for the most highly inbred
556 animals), we also calculated the cumulative probability for killer whales living to 40 years,
557 across the observed range of each F_{ROH} metric.
558 To understand the consequences of inbreeding depression on population viability, we first
559 calculated lifetime reproductive success for females. We first converted each draw of the
560 posterior distribution (logit space), to survival and fecundity rates, across the ranges of observed
561 F_{ROH} values. Second, for each potential F_{ROH} value, we simulated the lifetime reproductive
562 success of 20,000 random females; the survival and fecundity probabilities for those animals
563 were generated by randomly sampling from the posterior distribution of survival-at-age, and
564 fecundity-at-age, and stochastically simulating random birth and death events conditioned on
565 those probabilities. Mean lifetime reproductive success was then calculated as an average across
566 the 20,000 simulated females.
567 As a confirmation of the Bayesian modeling results, we also performed a simple linear
568 regression of age-at-death (years, for the 28 individuals that have died) as a function of F_{ROH} and
569 sex. As with the Bayesian modeling, animals with estimated birth years prior to 1960 were
570 excluded due to considerable uncertainty about birth years.

571 We used the statistical relationship between survival probability and H_{SNP} to estimate the
572 number of lethal equivalents for survival per haploid genome (b)[44] in the SRKW. b is typically
573 calculated as the negative log of the slope from a regression of the survival probability versus the
574 pedigree inbreeding coefficient[44,103]. b can also be estimated using genomic measures of
575 inbreeding such as F_{ROH} [45]. However, the minimum ROH length affects the range and variance
576 of F_{ROH} (Figures 1B, 1C) and can therefore strongly influence b. Individuals with the highest
577 $F_{ROH,10Mb}$ and F_{ROH1Mb} had a similar reduction in survival probability relative the least inbred
578 individuals in the population (Extended Data Figures 3-6), which would yield an estimate of b
579 that is larger when based on $F_{ROH,10Mb}$ instead of $F_{ROH,1Mb}$. We believe this difference is more

likely a technical artefact rather than an informative biological signal. We therefore estimated b from our analysis of inbreeding depression based on H_{SNP}, which accounts for all of the variation in inbreeding among individuals within the population and does not involve setting arbitrary minimum ROH length. First, we converted H_{SNP} into a heterozygosity-based metric of individual inbreeding (F_h) as

$$F = \left(H_{SNP,0} - H\right)/H_{SNP,0}, \quad \text{eq. 3}$$

where $H_{SNP,0}$ is the largest observed value of H_{SNP} in the SRKW population. F_h therefore measures the proportional reduction in the heterozygosity of each individual relative to the most heterozygous individual in the population who is assumed to be non-inbred[8,104]. We calculated the number of haploid lethal equivalents[44] for survival as

$$b = -\log\left(\frac{S_{F_{h,max}}}{S_{F_{h,0}}}\right)/F_{h,max}, \quad \text{eq. 4.}$$

where $S_{F_{h,max}}$ is the estimated survival probability of an individual with the highest observed F_h ($F_{h,max}$ = 0.38) in the population, and $S_{F_{h,0}}$ is the estimated survival probability of an individual with $F_h = 0$[46].

Effects of Inbreeding Depression on Population Growth

We used the same individual-based SRKW population model described above, and implemented in R, to evaluate the effect of the estimated inbreeding depression on SRKW population growth. Our individual based simulation model integrates a genetically explicit model of inbreeding depression[4,105-108] into the demographic model developed previously to evaluate population viability of the SRKW[23].

The simulated organism in the source population was self-incompatible, hermaphroditic, and had non-overlapping generations (for computational efficiency), and mean fecundity of 4[4]. The population size followed the estimates of N_e (Figure 1D) for the most recent 150 historical generations, and had a constant N_e = 587 (the estimate of N_e for 150 generations ago) for the previous 850 generations. Note that N_e = 587 is similar to a coalescent-based estimate of N_e for resident killer whales 10,000 years (~400 generations) ago[31]. After the source population simulation ran for 1,000 generations, we simulated the pedigree of individuals in the current

609 SRKW population in order to account for known ancestors and relationships among individuals.
610 Each individual whose parents were unknown (e.g., the pedigree 'founders') was randomly
611 assigned a diploid genome from the source population. We then projected the population into the
612 future, assuming a constant environment by using age- and sex-specific vital rates from year
613 2000. We chose year 2000 as the environmental reference year because the conditions were
614 approximately average then compared to the timespan of the study since the 1970s. The
615 simulations therefore assume vital rates that are likely inflated relative to current and possibly
616 future environmental conditions.
617 We ran 200 simulations of future population dynamics, accounting for inbreeding
618 depression by using a genetically-explicit model of deleterious genetic effects on survival as
619 described below. We compared the results from these simulations to 200 additional simulation
620 replicates where every individual was assigned the age- and sex-specific survival rates associated
621 with the lowest observed inbreeding among the SRKW in our statistical analysis of inbreeding
622 depression. This was done to isolate the effects of inbreeding depression on population growth
623 and viability. Each simulation replicate ran for either 100 years or until the population consisted
624 of <2 individuals, at which point the population was assumed extinct and population size was set
625 to zero.
626
627 *Genomic parameters*: The simulated genome had 20 chromosome pairs, each with an arbitrary
628 physical length of 10 Mb, and a genetic length of 50 centiMorgans. Haploid genomes from each
629 diploid parent were transmitted to diploid offspring assuming Mendelian segregation and random
630 distribution of recombination events across each chromosome.
631 We intentionally only model the inbreeding depression (i.e., effects of segregating
632 deleterious alleles) on survival that we detected in our empirical analysis, and ignore undetected
633 effects on other fitness components including fecundity and mortality before or shortly after
634 birth. Our approach is therefore conservative with respect to the demographic impact of
635 inbreeding depression. The simulation model assumes the sex-averaged haploid lethal
636 equivalents for survival to 40 years observed in our empirical analysis of survival as a function
637 of H_{SNP} as described above (b = 3.24).
638 Deleterious mutations were assigned physical locations randomly across the genome. We
639 set the mutation rate (/bp/generation) sufficiently high under several mutation models (see

below) to reliably yield substantially more deleterious mutations at the end of the source population simulation than needed to model inbreeding depression consistent with our empirical results. After simulating the source population, we calculated haploid lethal equivalents as

$$b = \sum_{i=1}^{L} q_i s_i - \sum_{i=1}^{L} q_i^2 s_i - 2\sum_{i=1}^{L}(q_i[1-q_i]s_i h_i), \qquad \text{eq. 5}$$

where s_i is the selection coefficient (the expected reduction in probability of surviving to 40 years for an individual homozygous for the derived allele relative to an individual homozygous for the ancestral allele) for the i^{th} of L simulated loci, q_i is the frequency of the deleterious derived allele at the i^{th} locus, and h is the dominance coefficient[103]. We then iteratively removed one randomly selected locus at a time until b for annual survival to 40 years was ≤ 3.24 in order to evaluate the effects of the inbreeding depression we detected in the SRKW on population growth over 100 years, beginning with a population with the same age and sex distributions of as the current SRKW population.

Empirical studies of mutation accumulation lines, humans, and non-model organisms have found that the size s (see eq. 5) is generally bimodally distributed, with the great majority of mutations following a gamma distribution and having relatively small fitness effects, and a minority of mutations being lethal or nearly lethal[109-113]. The results in Figure 2B are based on a model that assumes s was gamma distributed with shape parameter = 0.2 and scale parameter = 0.1 (Supplementary Figure 12). In order to include lethal mutations, which contribute substantially to inbreeding depression[4,9], we changed s to 1 for 2% of mutations. The dominance coefficient (h) declined exponentially with increasing size of s for deleterious alleles (i.e., mutations with larger s are more recessive) according to empirical data: $h = 0.5e^{-13s}$ [4,114] (Supplementary Figure 12).

The genetic component of fitness of simulated individual i in our simulations is summarized by the parameter w:

$$w_i = \prod_{j=1}^{n} 1 - \eta_{i,j} \begin{cases} h_j s_j & \text{if } \eta_{i,j}=1 \\ s_j & \text{if } \eta_{i,j}=0 \text{ or } 2 \end{cases}, \qquad \text{eq. 6}$$

where $\eta_{i,j}$ is the number of the derived deleterious alleles found at the j^{th} of the n polymorphic loci with a deleterious allele[4]. The simulated loci are assumed to have independent, multiplicative fitness effects[44]. We designated the highest observed value of w in the current population (e.g., year zero in Figure 2B, Extended Data Figure 9) as a reference intrinsic fitness (φ). We then calculate the probability of an age 1 individual (i) surviving over one year as

$$S_i = S_0 \left(\frac{w_i}{\varphi}\right)^{1/39}, \quad \text{eq. 7}$$

where S_0 is the empirically observed sex- and age-specific survival probability of a minimally-inbred individual surviving to 40 years (including effects of fixed deleterious alleles). The ratio $\frac{w_i}{\varphi}$ is raised to 1/39 to convert cumulative survival probability to 40 years to annual survival probability under the assumption that inbreeding depression for survival is constant across age classes. Importantly, the resulting simulated relationship between survival and inbreeding (Supplementary Figure 17) replicates the empirically observed inbreeding depression (Extended Data Figure 6). We then model mutation, Mendelian segregation, and selection in the SRKW through time, accounting for the demographic parameters for the population described above[23]. At year zero (i.e., the left end of the x-axis in Figure 2B), the mutation rate /bp/generation was set so that the average diploid offspring would carry one new deleterious mutation[4]. The flowchart in Supplementary Figure 18 summarizes the demographic simulation model.

We ran 14 sets of simulations in addition to those represented in Figure 2B to evaluate the effects of the assumed mutation parameters (Supplementary Table 15) on the population dynamics. We varied the shape of the distribution of *s* (changing the scale gamma parameter to 0.1 or 0.05), increased the rate at which *h* declines with increasing *s* ($h = 0.5e^{-50s}$), reduced the percentage of mutations that were lethal to either 0% or 1%, and set the deleterious mutation rate to zero starting in the first year of the simulation of future population dynamics (i.e., year zero in Figure 2B) to evaluate whether contemporary mutations affect the population dynamics. Finally, we implemented non-genetically explicit model where survival probability was a simple function of individual inbreeding, following Morton et al's[44] classical model of inbreeding depression. All of these alternative models (Supplementary Table 15) yielded qualitatively identical results to those shown in Fig. 2B (Extended Data Figure 9).

Data availability

Raw sequence data, and our killer whale genome assembly are freely available at the China National GeneBank DataBase (CNGBdb) with accession number CNP0002439 (https://db.cngb.org/search/project/CNP0002439/). Demographic data for the Southern Resident killer whales are freely available at https://doi.org/10.5281/zenodo.7011243. Other freely available reference genomes used here include Indo-Pacific dolphin

(https://www.ncbi.nlm.nih.gov/assembly/GCA_003227395.1), North Atlantic right whale (https://www.dnazoo.org/assemblies/Eubalaena_glacialis), and Pacific white-sided dolphin (https://www.dnazoo.org/assemblies/Lagenorhynchus_obliquidens).

Code availability

Computer code used in this study is available at https://doi.org/10.5281/zenodo.7504838.

Acknowledgements

We are grateful to Phil Levin, Xinying Zeng, Yiwu He and Yuhan Zhang for facilitating this project. This project would not have been possible without the long-term monitoring of the SRKW population provided by Ken Balcomb and the Center for Whale Research, WA. The China National GeneBank provided technical support with sequence data. The North Gulf Oceanic Society provided DNA from Alaska resident killer whales. Funding was provided by the National Natural Science Foundation of China (Grant numbers 42225604 and 41422604), "One Belt and One Road" Science and Technology Cooperation Special Program of the International Partnership Program of the Chinese Academy of Sciences (183446KYSB20200016), and Blue granary scientific and technological innovation of China (2018YFD0900301-05).

Author contributions

MJF, KMP, GF and SL initiated the study. COM, MBH, CE, SL planned and conducted fieldwork and provided samples. YZ, PZ, HK, XX, XL, and YA assembled the genome and conducted population structure analyses. YZ, PZ, HK, XX, XL, YA, and MK conducted bioinformatics. MK conducted analyses of demographic history and inbreeding. MK and EJW conducted inbreeding depression and demographic projection analyses. MK, MJF, YZ, KMP and YA wrote the first draft of the paper, and all authors commented and contributed to the final draft.

Competing Interests

The authors declare no competing interests.

Tables

Table 1. Results from Bayesian logistic regression analysis of the effects of F_{ROH} and H_{SNP} on annual survival. Posterior means, 95% posterior credible intervals, and probability of negative values of the $B_{F_{ROH}}$ and $B_{H_{SNP}}$ parameters. Individuals included in these analyses are in Supplementary Table 8 (85 animals, using 2,169 animal-year observations). Increasing inbreeding (F_{ROH}) is associated with decreasing heterozygosity (H_{SNP}), so the regression coefficients for F_{ROH} and H_{SNP} have opposite signs.

Model	Mean	Lower 95%	Upper 95%	Pr(< 0)
$F_{ROH,1Mb}$	-0.395	-0.773	-0.004	0.976
$F_{ROH,10Mb}$	-0.363	-0.724	0.011	0.972
H_{SNP}	0.429	0.060	0.796	0.012

Figure Legends

Figure 1. Distribution, population structure, inbreeding, and demographic history for five North Pacific killer whale populations. (**A**) Geographic population distributions, with inset showing population genetic structure in a neighbor joining tree and admixture analysis (Extended Data Figure 1). (**B**) The distributions of $F_{ROH,1Mb}$, and (**C**) $F_{ROH,10Mb}$. Point estimates and 95% bootstrap confidence intervals for mean F_{ROH} are shown to the right of B and C for each population (n=100 [Southern Residents], n=24 [Alaska Residents], n=14 [Transients]) except the Northern Residents due to the small sample size (n=2). (**D**) Historical N_e estimates (thick lines) with 95% (light shaded regions) and 50% (dark shaded regions) confidence intervals over the last >150 generations were estimated from patterns of linkage disequilibrium (LD) among linked SNPs[35]. (**E**) Estimates and 95% confidence intervals for contemporary N_e were derived from patterns of LD between loci on separate chromosomes[36]. Analyses in D and E are based on samples sizes of n=75 (Southern Residents), n=19 (Alaska Residents), n=13 (Transients). Population structure methods are available in the Supplementary Methods.

Figure 2. Effects of inbreeding on survival to age 40 years and population growth. (**A**) The relationship between survival probability to age 40 and $F_{ROH,10Mb}$. The thin blue lines represent 5,000 random MCMC draws of the estimated relationship between survival and $F_{ROH,10Mb}$ in our Bayesian model. The thick blue line is the median, and the shaded areas are the central 50% (dark) and 95% (light) of the 5,000 random MCMC draw estimates. (**B**) Projected future population trends are shown with (red) and without (gray) inbreeding depression. Each thin line represents one of 200 independent simulation replicates. Thick lines represent the median, and the shaded areas represent the central 50% (dark) and 95% (light) of population size through time across the 200 simulation replicates.

Figure 3. Genetic loads in North Pacific killer whales. (**A**) Pairwise comparisons of the abundance of loss-of-function and missense mutations ($R_{X/Y}$) among SRKW (Southern Resident, n=12), ARKW (Alaska Resident, n=12), and TKW (Transient, n=12) populations. $R_{X/Y}>1$ and $R_{X/Y}<1$ mean that deleterious alleles are more or less abundant, respectively, in population X than in population Y. Solid points are point estimates, and error bars represent the standard deviation among 100 block jackknife samples of the data[56] (**B)** The homozygous mutation load (number of homozygous, putatively deleterious alleles) versus $F_{ROH,1Mb}$. Linear regression lines are included for populations with a sample size >10. The pattern shown is similar when homozygous mutation load is plotted against H_{SNP}, and when only LOF alleles were used to estimate the homozygous mutation load (Supplementary Figures 10-11). (**C**) The total homozygous mutation load for each individual (colored points), and its population mean (orange points, +/- 1 s.d.) partitioned between homozygous genotypes due to fixed deleterious alleles (hatched bars), versus loci that were polymorphic for putatively deleterious alleles (solid bars). Sample sizes in B and C are n=100 (SRKW), n=24 (ARKW), n=7 (Offshore), and n=14 (TKW).

References

1. Urban, M.C. Accelerating extinction risk from climate change. *Science* **348**, 571-573 (2015).
2. Caughley, G. Directions in conservation biology. *Journal of Animal Ecology*, 215-244 (1994).
3. Hedrick, P.W., Lacy, R.C., Allendorf, F.W. & Soulé, M.E. Directions in conservation biology: comments on Caughley. *Conservation Biology* **10**, 1312-1320 (1996).
4. Kardos, M. *et al.* The crucial role of genome-wide genetic variation in conservation. *Proceedings of the National Academy of Sciences* **118**, e2104642118 (2021).
5. O'Grady, J.J. *et al.* Realistic levels of inbreeding depression strongly affect extinction risk in wild populations. *Biological Conservation* **133**, 42-51 (2006).
6. Shaffer, M.L. Minimum population sizes for species conservation. *BioScience* **31**, 131-134 (1981).
7. Soulé, M.E. *Viable Populations for Conservation*, (Cambridge University Press, 1987).
8. Kardos, M., Taylor, H.R., Ellegren, H., Luikart, G. & Allendorf, F.W. Genomics advances the study of inbreeding depression in the wild. *Evolutionary Applications* **9**, 1205-1218 (2016).
9. Charlesworth, D. & Willis, J.H. The genetics of inbreeding depression. *Nature Reviews Genetics* **10**, 783-796 (2009).
10. Keller, L.F. & Waller, D.M. Inbreeding effects in wild populations. *Trends in Ecology & Evolution* **17**, 230-241 (2002).
11. Ralls, K., Brugger, K. & Ballou, J. Inbreeding and juvenile mortality in small populations of ungulates. *Science* **206**, 1101-3 (1979).

12. Whiteley, A.R., Fitzpatrick, S.W., Funk, W.C. & Tallmon, D.A. Genetic rescue to the rescue. *Trends in Ecology & Evolution* **30**, 42-49 (2015).
13. Robinson, Z.L. *et al.* Experimental test of genetic rescue in isolated populations of brook trout. *Molecular Ecology* **26**, 4418-4433 (2017).
14. Bozzuto, C., Biebach, I., Muff, S., Ives, A.R. & Keller, L.F. Inbreeding reduces long-term growth of Alpine ibex populations. *Nature Ecology & Evolution* **3**, 1359-1364 (2019).
15. Saccheri, I. *et al.* Inbreeding and extinction in a butterfly metapopulation. *Nature* **392**, 491-494 (1998).
16. Teixeira, J.C. & Huber, C.D. The inflated significance of neutral genetic diversity in conservation genetics. *Proceedings of the National Academy of Sciences* **118**, e2015096118 (2021).
17. Ford, J.K. *et al.* Dietary specialization in two sympatric populations of killer whales (*Orcinus orca*) in coastal British Columbia and adjacent waters. *Canadian Journal of Zoology* **76**, 1456-1471 (1998).
18. Dahlheim, M. *et al.* Eastern temperate North Pacific offshore killer whales (*Orcinus orca*): occurrence, movements, and insights into feeding ecology. *Marine Mammal Science* **24**, 719-729 (2008).
19. Ford, J.K. *et al.* Shark predation and tooth wear in a population of northeastern Pacific killer whales. *Aquatic Biology* **11**, 213-224 (2011).
20. Parsons, K.M. *et al.* Geographic patterns of genetic differentiation among killer whales in the northern North Pacific. *Journal of Heredity* **104**, 737-754 (2013).
21. Olesiuk, P., Bigg, M. & Ellis, G. Life history and population dynamics of resident killer whales (*Orcinus orca*) in the coastal waters of British Columbia and Washington State. *Report of the International Whaling Commission (Special Issue 12)* **12**, 209-43 (1990).
22. Cosewic. COSEWIC assessment and update status report on the killer whale *Orcinus orca*, Southern Resident population, Northern Resident population, West Coast Transient population, Offshore population and Northwest Atlantic/Eastern Arctic population, in Canada. *Committee on the Status of Endangered Wildlife in Canada*, viii+-65 (2008).
23. Ward, E.J., M.J. Ford, R.G. Kope, J.K.B. Ford, L.A. VelezEspino, C.K. Parken, L.W. LaVoy, M.B. Hanson, and K.C. Balcomb. Estimating the impacts of Chinook salmon abundance and prey removal by ocean fishing on Southern Resident killer whale population dynamics. U.S. Dept. Commer., NOAA Tech. Memo. NMFS-NWFSC-123 (2013).
24. National Marine Fisheries Service. Recovery plan for Southern Resident killer whales (*Orcinus orca*). (National Marine Fisheries Service, Northwest Region, Seattle, WA, 2008).
25. Kirin, M. *et al.* Genomic runs of homozygosity record population history and consanguinity. *Plos One* **5**, e13996 (2010).
26. Ceballos, F.C., Joshi, P.K., Clark, D.W., Ramsay, M. & Wilson, J.F. Runs of homozygosity: windows into population history and trait architecture. *Nature Reviews Genetics* **19**, 220-234 (2018).
27. Kardos, M., Qvarnström, A. & Ellegren, H. Inferring individual inbreeding and demographic history from segments of identity by descent in *Ficedula* flycatcher genome sequences. *Genetics* **205**, 1319-1334 (2017).
28. Thompson, E.A. Identity by descent: variation in meiosis, across genomes, and in

865 populations. *Genetics* **194**, 301-326 (2013).
866 29. Stoffel, M.A., Johnston, S.E., Pilkington, J.G. & Pemberton, J.M. Mutation load
867 decreases with haplotype age in wild Soay sheep. *Evolution Letters* **5**, 187-195 (2021).
868 30. Szpiech, Z.A. *et al.* Long runs of homozygosity are enriched for deleterious variation.
869 *The American Journal of Human Genetics* **93**, 90-102 (2013).
870 31. Foote, A.D. *et al.* Runs of homozygosity in killer whale genomes provide a global record
871 of demographic histories. *Molecular Ecology* **30**, 6162-6177 (2021).
872 32. Barrett-Lennard, L.G. & Ellis, G. Population structure and genetic variability in
873 northeastern Pacific killer whales: towards an assessment of population viability.
874 Department of Fisheries and Oceans Canada, Research Document 2001/65. (2001).
875 33. Ford, M.J. *et al.* Inbreeding in an endangered killer whale population. *Animal*
876 *Conservation* **21**, 423-432 (2018).
877 34. Ford, M.J. *et al.* Inferred paternity and male reproductive success in a killer whale
878 (*Orcinus orca*) population. *Journal of Heredity* **102**, 537-553 (2011).
879 35. Santiago, E. *et al.* Recent demographic history inferred by high-resolution analysis of
880 linkage disequilibrium. *Molecular Biology and Evolution* **37**, 3642-3653 (2020).
881 36. Do, C. *et al.* NeEstimator v2: re-implementation of software for the estimation of
882 contemporary effective population size (N_e) from genetic data. *Molecular Ecology*
883 *Resources* **14**, 209-214 (2014).
884 37. Waples, R.S. Genetic methods for estimating the effective size of cetacean populations.
885 *Report of the International Whaling Commission (special issue)* **13**, 279-300 (1991).
886 38. Robinson, J.A. *et al.* Genomic flatlining in the endangered island fox. *Current Biology*
887 **26**, 1183-1189 (2016).
888 39. Hedrick, P., Robinson, J., Peterson, R.O. & Vucetich, J.A. Genetics and extinction and the
889 example of Isle Royale wolves. *Animal Conservation* **22**, 302-309 (2019).
890 40. Dussex, N. *et al.* Population genomics of the critically endangered kākāpō. *Cell*
891 *Genomics*, 100002 (2021).
892 41. Kardos, M. *et al.* Genomic consequences of intensive inbreeding in an isolated wolf
893 population *Nature Ecology & Evolution* **2**, 124-131 (2018).
894 42. Robinson, J.A. *et al.* Genomic signatures of extensive inbreeding in Isle Royale wolves, a
895 population on the threshold of extinction. *Science Advances* **5**, eaau0757 (2019).
896 43. Hoelzel, A.R. *et al.* Evolution of population structure in a highly social top predator, the
897 killer whale. *Molecular Biology and Evolution* **24**, 1407-1415 (2007).
898 44. Morton, N.E., Crow, J.F. & Muller, H.J. An estimate of the mutational damage in man
899 from data on consanguineous marriages. *Proceedings of the National Academy of*
900 *Sciences* **42**, 855-863 (1956).
901 45. Stoffel, M.A., Johnston, S.E., Pilkington, J.G. & Pemberton, J.M. Genetic architecture
902 and lifetime dynamics of inbreeding depression in a wild mammal. *Nature*
903 *Communications* **12**, 1-10 (2021).
904 46. Charlesworth, D. & Charlesworth, B. Inbreeding depression and its evolutionary
905 consequences. *Annual Review of Ecology and Systematics* **18**, 237-268 (1987).
906 47. Ralls, K., Ballou, J.D., Rideout, B.A. & Frankham, R. Genetic management of
907 chondrodystrophy in California condors. *Animal Conservation* **3**, 145-153 (2000).
908 48. McCune, A.R. *et al.* A low genomic number of recessive lethals in natural populations of
909 bluefin killifish and zebrafish. *Science* **296**, 2398-2401 (2002).
910 49. Wasser, S.K. *et al.* Population growth is limited by nutritional impacts on pregnancy

success in endangered Southern Resident killer whales (*Orcinus orca*). *PLoS One* **12**, e0179824 (2017).
50. Hedrick, P.W. & Garcia-Dorado, A. Understanding inbreeding depression, purging, and genetic rescue. *Trends in Ecology & Evolution* **31**, 940-952 (2016).
51. Muto, M. *et al.* Alaska marine mammal stock assessments, 2016. (ed. Service, N.M.F.) (National Marine Fisheries Service, 2017).

52. Holt, M.M. *et al.* Vessels and their sounds reduce prey capture effort by endangered killer whales (*Orcinus orca*). *Marine Environmental Research* **170**, 105429 (2021).
53. Ford, J.K., Ellis, G.M., Olesiuk, P.F. & Balcomb, K.C. Linking killer whale survival and prey abundance: food limitation in the oceans' apex predator? *Biology Letters* **6**, 139-142 (2010).
54. Krahn, M.M. *et al.* Persistent organic pollutants and stable isotopes in biopsy samples (2004/2006) from Southern Resident killer whales. *Marine Pollution Bulletin* **54**, 1903-1911 (2007).
55. McLaren, W. *et al.* The ensembl variant effect predictor. *Genome Biology* **17**, 1-14 (2016).
56. Do, R. *et al.* No evidence that selection has been less effective at removing deleterious mutations in Europeans than in Africans. *Nature Genetics* **47**, 126-131 (2015).
57. Khan, A. *et al.* Genomic evidence for inbreeding depression and purging of deleterious genetic variation in Indian tigers. *Proceedings of the National Academty of Sciences* **118**, e2023018118 (2021).
58. Matkin, C.O., Ward Testa, J., Ellis, G.M. & Saulitis, E.L. Life history and population dynamics of southern Alaska resident killer whales (*Orcinus orca*). *Marine Mammal Science* **30**, 460-479 (2014).
59. National Marine Fisheries Service. Southern Resident Killer Whales (*Orcinus orca*) 5-Year Review: Summary and Evaluation. (National Marine Fisheries Service West Coast Region Seattle, WA, 2016).
60. Xue, Y. *et al.* Mountain gorilla genomes reveal the impact of long-term population decline and inbreeding. *Science* **348**, 242-245 (2015).
61. Robinson, J.A., Brown, C., Kim, B.Y., Lohmueller, K.E. & Wayne, R.K. Purging of strongly deleterious mutations explains long-term persistence and absence of inbreeding depression in island foxes. *Current Biology* **28**, 3487-3494. e4 (2018).
62. Grossen, C., Guillaume, F., Keller, L.F. & Croll, D. Purging of highly deleterious mutations through severe bottlenecks in Alpine ibex. *Nature Communications* **11**, 1-12 (2020).
63. Robinson, J.A. *et al.* The critically endangered vaquita is not doomed to extinction by inbreeding depression. *Science* **376**, 635-639 (2022).
64. Robinson, J., Kyriazis, C.C., Yuan, S.C. & Lohmueller, K.E. Deleterious variation in natural populations and implications for conservation genetics. *Annual Review of Animal Biosciences* **11**(2022).
65. García-Dorado, A. Understanding and predicting the fitness decline of shrunk populations: inbreeding, purging, mutation, and standard selection. *Genetics* **190**, 1461-1476 (2012).
66. Kijas, J.W. *et al.* Genome-wide analysis of the world's sheep breeds reveals high levels of historic mixture and strong recent selection. *PLoS Biol* **10**, e1001258 (2012).

67. Clutton-Brock, T.H. & Pemberton, J.M. *Soay sheep: dynamics and selection in an island population*, (Cambridge University Press, 2004).
68. Garcia-Dorado, A. & Hedrick, P. Some hope and many concerns on the future of the vaquita. *Heredity*, 1-4 (2022).
69. Huisman, J., L.E.B, K., P.A., E., Clutton-Brock, T. & Pemberton, J.M. Inbreeding depression across the lifespan in a wild mammal population. *Proceedings of the National Academy of Sciences* **113**, 3585-3590 (2016).
70. Nelms, S.E. *et al.* Marine mammal conservation: over the horizon. *Endangered Species Research* **44**, 291-325 (2021).
71. Avila, I.C., Kaschner, K. & Dormann, C.F. Current global risks to marine mammals: taking stock of the threats. *Biological Conservation* **221**, 44-58 (2018).
72. Ward, E.J., Holmes, E.E. & Balcomb, K.C. Quantifying the effects of prey abundance on killer whale reproduction. *Journal of Applied Ecology* **46**, 632-640 (2009).
73. Myers, H.J., Olsen, D.W., Matkin, C.O., Horstmann, L.A. & Konar, B. Passive acoustic monitoring of killer whales (*Orcinus orca*) reveals year-round distribution and residency patterns in the Gulf of Alaska. *Scientific Reports* **11**, 1-14 (2021).
74. Snyder, R.E. How demographic stochasticity can slow biological invasions. *Ecology* **84**, 1333-1339 (2003).
75. Brown, J.H. On the relationship between abundance and distribution of species. *The American Naturalist* **124**, 255-279 (1984).
76. Ward, E. *et al.* Long‐distance migration of prey synchronizes demographic rates of top predators across broad spatial scales. *Ecosphere* **7**, e01276 (2016).
77. Ford, J.K.B., Wright, B.M., Ellis, G.M. & Candy, J.R. *Chinook salmon predation by resident killer whales: seasonal and regional selectivity, stock identity of prey, and consumption rates*, (Canadian Science Advisory Secretariat; Secrétariat canadien de consultation …, 2010).
78. Chasco, B.E. *et al.* Competing tradeoffs between increasing marine mammal predation and fisheries harvest of Chinook salmon. *Scientific Reports* **7**, 1-14 (2017).
79. Beck, S. *et al.* Using opportunistic photo-identifications to detect a population decline of killer whales (*Orcinus orca*) in British and Irish waters. *Journal of the Marine Biological Association of the United Kingdom* **94**, 1327-1333 (2014).
80. Carretta, J.V. *et al.* US Pacific marine mammal stock assessments: 2021. U.S. Department of Commerce. *NOAA Technical Memorandum NMFS-SWFSC* **663** (2022).
81. Muto, M. *et al.* Alaska marine mammal stock assessments: 2019. US Department of Commerce. *NOAA Technical Memorandum NMFS-AFSC* **404**(2020).
82. Thomas, J.C., Khoury, R., Neeley, C.K., Akroush, A.M. & Davies, E.C. A fast CTAB method of human DNA isolation for polymerase chain reaction applications. *Biochemical Education* **25**, 233-235 (1997).
83. Bigg, M.A. *Killer whales: a study of their identification, genealogy, and natural history in British Columbia and Washington State*, (Nanaimo, BC: Phantom, 1987).
84. Center for Whale Research. *Southern Resident Killer Whale ID Guide*, (Center for Whale Research, Friday Harbor, WA, USA., 2022).
85. Sambrook, J. & Russell, D. *Molecular Cloning: A Laboratory Manual*, (Woodbury, New York, 2000).
86. Chen, Y. *et al.* SOAPnuke: a MapReduce acceleration-supported software for integrated quality control and preprocessing of high-throughput sequencing data. *GigaScience* **7**,

gix120 (2017).
87. Walker, B.J. *et al.* Pilon: an integrated tool for comprehensive microbial variant detection and genome assembly improvement. *PloS One* **9**, e112963 (2014).
88. Servant, N. *et al.* HiC-Pro: an optimized and flexible pipeline for Hi-C data processing. *Genome Biology* **16**, 1-11 (2015).
89. Dudchenko, O. *et al.* De novo assembly of the Aedes aegypti genome using Hi-C yields chromosome-length scaffolds. *Science* **356**, 92-95 (2017).
90. Foote, A.D. *et al.* Convergent evolution of the genomes of marine mammals. *Nature Genetics* **47**, 272-275 (2015).
91. Li, H. & Durbin, R. Fast and accurate long-read alignment with Burrows-Wheeler transform. *Bioinformatics* **26**, 589-95 (2010).
92. Guindon, S., Delsuc, F., Dufayard, J.-F. & Gascuel, O. Estimating maximum likelihood phylogenies with PhyML. in *Bioinformatics for DNA Sequence Analysis* (ed. Posada, D.) 113-137 (Humana Press, New York City, 2009).
93. McKenna, A. *et al.* The Genome Analysis Toolkit: a MapReduce framework for analyzing next-generation DNA sequencing data. *Genome Research* **20**, 1297-1303 (2010).
94. Pemberton, T.J. *et al.* Genomic patterns of homozygosity in worldwide human populations. *The American Journal of Human Genetics* **91**, 275-292 (2012).
95. Quinlan, A.R. & Hall, I.M. BEDTools: a flexible suite of utilities for comparing genomic features. *Bioinformatics* **26**, 841-842 (2010).
96. Danecek, P. *et al.* Twelve years of SAMtools and BCFtools. *Gigascience* **10**, giab008 (2021).
97. Hilborn, R.S. *et al.* Reflections of the science panel from workshop 1 and guidance for workshop 2. Prepared with the assistance of ESSA Technologies Ltd., Vancouver, B.C. for National Marine Fisheries Service (Seattle WA) and Fisheries and Oceans Canada (Vancouver BC). 41 pp. (2011).
98. Bürkner, P.-C. brms: An R package for Bayesian multilevel models using Stan. *Journal of Statistical Software* **80**, 1-28 (2017).
99. Gabry, J. & Češnovar, R. Cmdstanr: R interface to 'CmdStan'. (2020).
100. Hoffman, M.D. & Gelman, A. The No-U-Turn sampler: adaptively setting path lengths in Hamiltonian Monte Carlo. *Journal of Machine Learning Research* **15**, 1593-1623 (2014).
101. Carpenter, B. *et al.* Stan: A probabilistic programming language. *Journal of Statistical Software* **76**, 1-32 (2017).
102. Vehtari, A., Gelman, A., Simpson, D., Carpenter, B. & Bürkner, P.-C. Rank-normalization, folding, and localization: An improved R-hat for assessing convergence of MCMC. *Bayesian Analysis* **16**, 667-718 (2021).
103. Nietlisbach, P., Muff, S., Reid, J.M., Whitlock, M.C. & Keller, L.F. Nonequivalent lethal equivalents: Models and inbreeding metrics for unbiased estimation of inbreeding load. *Evolutionary Applications* **12**, 266-279 (2019).
104. Crow, J.F. & Kimura, M. *An introduction to population genetics theory*, (Harper & Row, New York, 1970).
105. Kardos, M. & Luikart, G. The genetic architecture of fitness drives population viability during rapid environmental change. *The American Naturalist* **197**, 511-525 (2021).
106. Kardos, M., Luikart, G. & Allendorf, F.W. Measuring individual inbreeding in the age of genomics: marker-based measures are better than pedigrees. *Heredity* **115**, 63-72 (2015).

107. Kardos, M., Allendorf, F.W. & Luikart, G. Evaluating the role of inbreeding depression in heterozygosity-fitness correlations: how useful are tests for identity disequilibrium? *Molecular Ecology Resources* **14**, 519-530 (2014).
108. Robinson, Z.L. *et al.* Evaluating the outcomes of genetic rescue attempts. *Conservation Biology* **35**, 666-677 (2021).
109. Eyre-Walker, A. & Keightley, P.D. The distribution of fitness effects of new mutations. *Nature Reviews Genetics* **8**, 610-618 (2007).
110. Eyre-Walker, A., Woolfit, M. & Phelps, T. The distribution of fitness effects of new deleterious amino acid mutations in humans. *Genetics* **173**, 891-900 (2006).
111. Simmons, M.J. & Crow, J.F. Mutations affecting fitness in *Drosophila* populations. *Annual Review of Genetics* **11**, 49-78 (1977).
112. Ballinger, M.A. & Noor, M.A. Are lethal alleles too abundant in humans? *Trends in Genetics* **34**, 87-89 (2018).
113. Lacy, R.C., Alaks, G. & Walsh, A. Hierarchical analysis of inbreeding depression in *Peromyscus polionotus*. *Evolution* **50**, 2187-2200 (1996).
114. Deng, H.-W. & Lynch, M. Estimation of deleterious-mutation parameters in natural populations. *Genetics* **144**, 349-360 (1996).

Figure or Table # Please group Extended Data items by type, in sequential order. Total number of items (Figs. + Tables) must not exceed 10.	Figure/Table title One sentence only	Filename Whole original file name including extension. i.e.: Smith_ED_Fig1.jpg	Figure/Table Legend If you are citing a reference for the first time in these legends, please include all new references in the main text Methods References section, and carry on the numbering from the main References section of the paper. If your paper does not have a Methods section, include all new references at the end of the main Reference list.
Extended Data Fig. 1	Neighbor joining (NJ) tree and admixture analysis of killer whale population structure.	ExtendedData_Fig1.pdf	Neighbor joining (NJ) tree and admixture analysis of killer whale population structure. One false killer whale sample was used as the outgroup to construct the NJ tree.
Extended Data Fig. 2	Historical N_e estimates (thick lines) and 95% confidence intervals (shaded regions) over the last 50 generations were estimated from patterns of linkage disequilibrium (LD) among linked SNPs with the program GONE (*46*).	ExtendedData_Fig2.pdf	Historical N_e estimates (thick lines) and 95% confidence intervals (shaded regions) over the last 50 generations were estimated from patterns of linkage disequilibrium (LD) among linked SNPs with the program GONE (*46*). The results for all 150 generations are shown in Fig. 1D in the main text. Here we zoom in on the estimated effective sizes over the last 50 generations for Transient (green), Alaska Resident (dark blue), and Southern Resident (light blue) killer whales.
Extended Data Fig. 3	Annual survival estimates for an average 20-year-old, by sex, as a function of F_{ROH} values.	ExtendedData_Fig3.pdf	Annual survival estimates for an average 20-year-old, by sex, as a function of F_{ROH} values. The thin blue lines represent 5,000 random MCMC draws of the estimated relationship between survival and F_{ROH} in our Bayesian

			model. The thick solid lines represent the posterior mean. The shaded areas represent the central 50% (dark) and 95% (light) of survival probability across the 5,000 MCMC draws. These results can be compared directly to Fig. S19 which shows an increase in estimated annual survival as H_{SNP} increases.
Extended Data Fig. 4	Cumulative survival estimates to age 40, by sex, as a function of F_{ROH}.	ExtendedData_Fig4.pdf	Cumulative survival estimates to age 40, by sex, as a function of F_{ROH}. The thin blue lines represent 5,000 random MCMC draws of the estimated relationship between cumulative survival and F_{ROH} in our Bayesian model. The thick solid lines represent the posterior mean. The shaded areas represent the central 50% (dark) and 95% (light) of survival probability across the 5,000 MCMC draws. These results can be compared directly to Fig. S20 which shows an increase in estimated cumulative survival as H_{SNP} increases.
Extended Data Fig. 5	Annual survival estimates by sex, as a function of H_{SNP}.	ExtendedData_Fig5.pdf	Annual survival estimates by sex, as a function of H_{SNP}. The thin blue lines represent 5,000 random MCMC draws of the

			estimated relationship between cumulative survival and H_{SNP} in our Bayesian model. The thick solid lines represent the posterior mean. The shaded areas represent the central 50% (dark) and 95% (light) of survival probability across the 5,000 MCMC draws. These results can be compared directly to Fig. S17 which shows a decrease in estimated annual survival as F_{ROH} increases.
Extended Data Fig. 6	Cumulative survival estimates to age 40, by sex, as a function of H_{SNP}.	ExtendedData_Fig6.pdf	Cumulative survival estimates to age 40, by sex, as a function of H_{SNP}. The thin blue lines represent 5,000 random MCMC draws of the estimated relationship between cumulative survival and H_{SNP} in our Bayesian model. The thick solid lines represent the posterior mean. The shaded areas represent the central 50% (dark) and 95% (light) of survival probability across the 5,000 MCMC draws. These results can be compared directly to Fig. S18 which shows a decrease in estimated cumulative survival as F_{ROH} increases.
Extended Data Fig. 7	Relationship of age at death with F_{ROH} and sex. Relationship between F_{ROH} and age	ExtendedData_Fig7.pdf	Relationship of age at death with F_{ROH} and sex. Relationship between F_{ROH} and age at death is

	at death is shown for analyses using minimum ROH lengths of 1 Mb (A) and 10 Mb (B) for females (left) and males (right).		shown for analyses using minimum ROH lengths of 1 Mb (A) and 10 Mb (B) for females (left) and males (right). Solid lines are fitted values from the statistical results shown in Supplementary Table 14. The model is of the form $\text{Age} = B_0 + B_{F_{\text{ROH}}} + \text{sex}$, and the fitted lines shown in the plots have sex-specific intercepts according to the output (Supplementary Table 14). This analysis is based on the 28 SRKW individuals with sequence data that have died over the course of the study.
Extended Data Fig. 8	Lifetime reproductive success for SRKW females, calculated via the age-based models in our analysis plotted against F_{ROH}.killer whale population under models 1-15 (Supplementary Table 15).	ExtendedData_Fig8.pdf	Lifetime reproductive success for SRKW females, calculated via the age-based models in our analysis plotted against F_{ROH}. F_{ROH} was measured using ROH with minimum lengths of 1 Mb and 10 Mb (different colored lines as indicated in the legend).
Extended Data Fig. 9	Simulated future population trends with (red) and without (gray) inbreeding depression in the Southern Resident killer whale population under models 1-15 (Supplementary Table 15).	ExtendedData_Fig9.pdf	Simulated future population trends with (red) and without (gray) inbreeding depression in the Southern Resident killer whale population under models 1-15 (Supplementary Table 15). Each thin line represents one of 200 simulation replicates. Thick lines represent the median projected population size through

			time. The shaded areas represent the central 50% (dark) and 95% (light) of population size.
Extended Data Fig. 10	Site-frequency spectra based on analysis of 12 individual genomes from the Southern Resident (left), Alaska Resident (middle), and Transient killer whales (right).	ExtendedData_Fig10.pdf	Site-frequency spectra based on analysis of 12 individual genomes from the Southern Resident (left), Alaska Resident (middle), and Transient killer whales (right). The SFS for putatively deleterious and neutral are shown as blue and orange lines, respectively. Derived allele frequencies of 0 and 1 are excluded.

1

Item	Present?	Filename Whole original file name including extension. i.e.: Smith_SI.pdf. The extension must be .pdf	A brief, numerical description of file contents. i.e.: *Supplementary Figures 1-4, Supplementary Discussion, and Supplementary Tables 1-4.*
Supplementary Information	Yes	Orca_Supplement_4January2023.pdf	Supplementary Methods, Supplementary Figures 1-18, Supplementary Tables 1-16
Reporting Summary	Yes	nr-reporting-summary_ORCA_MK_5January2023.pdf	
Peer Review Information	Yes	*Kardos_PRfile.pdf*	

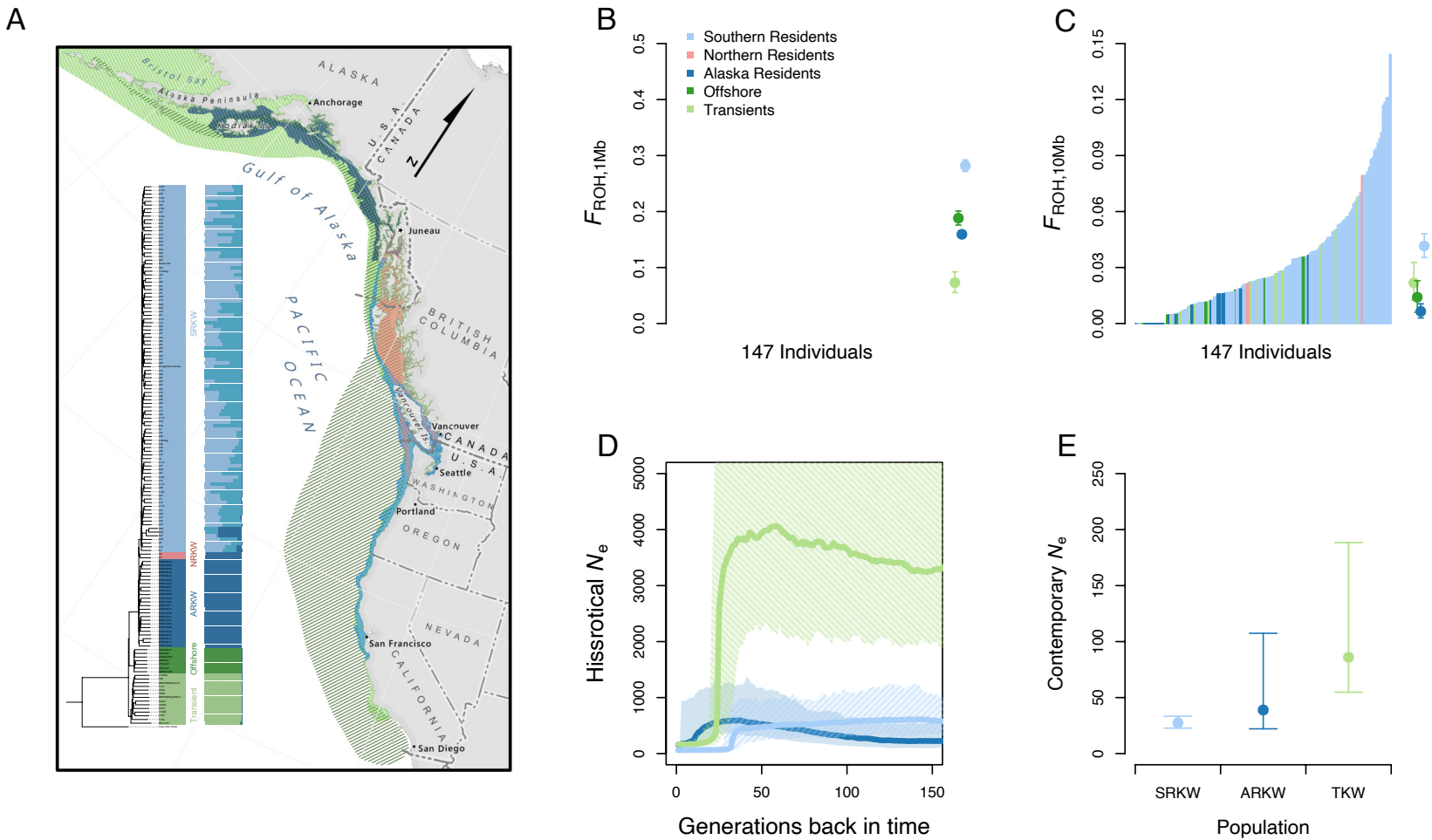
A
ALASKA
Bristol Bay
Alaska Peninsula
Kodiak Is.
Anchorage
U.S.A.
CANADA
N
Gulf of Alaska
Juneau
PACIFIC OCEAN
BRITISH COLUMBIA
Vancouver
CANADA
U.S.A.
Seattle
WASHINGTON
Portland
OREGON
NEVADA
San Francisco
CALIFORNIA
San Diego
SRKW
NRKW
ARKW
Offshore
Transient
B
Southern Residents
Northern Residents
Alaska Residents
Offshore
Transients
$F_{ROH,1Mb}$
0.0
0.1
0.2
0.3
0.4
0.5
147 Individuals
C
$F_{ROH,10Mb}$
0.00
0.03
0.06
0.09
0.12
0.15
147 Individuals
D
Hissrotical N_e
0
1000
2000
3000
4000
5000
0
50
100
150
Generations back in time
E
Contemporary N_e
0
50
100
150
200
250
SRKW
ARKW
TKW
Population

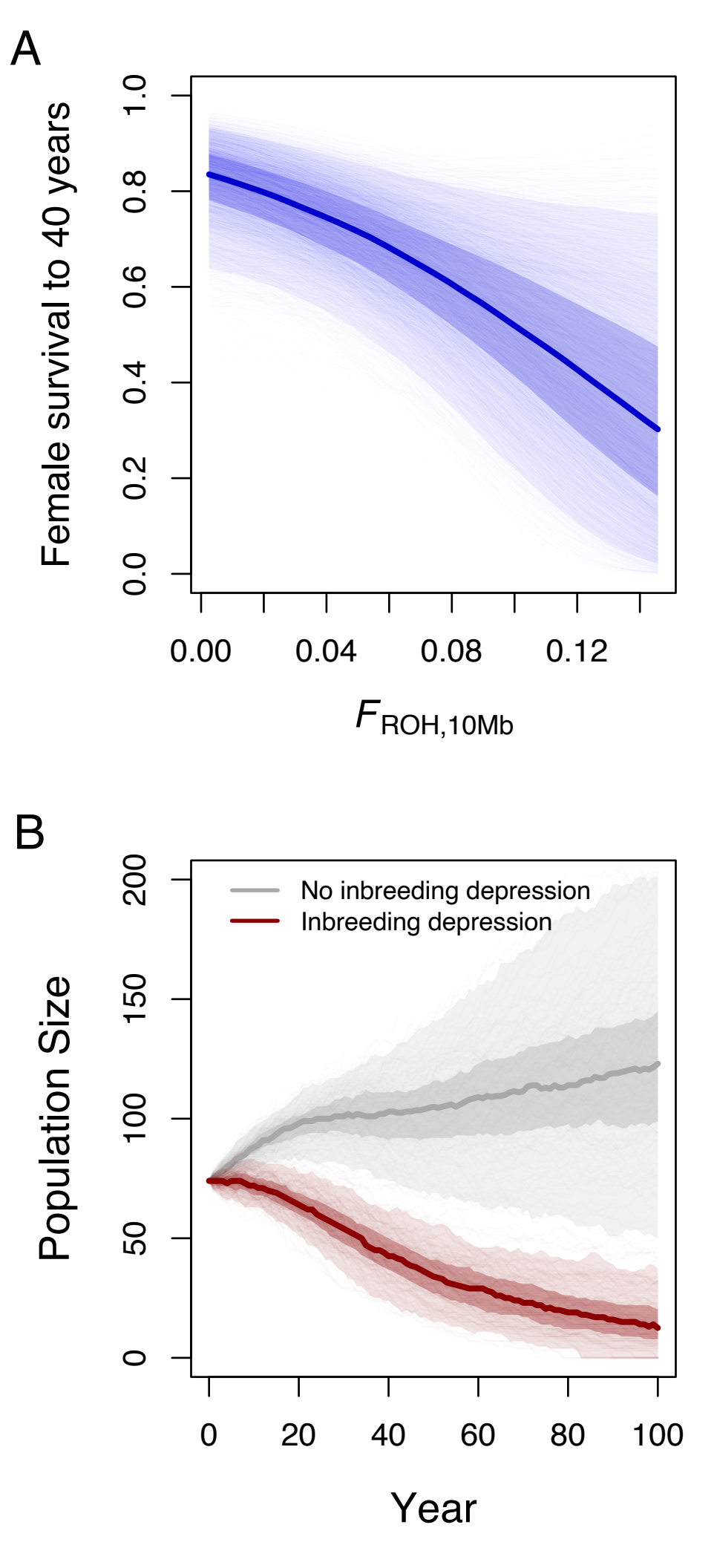
A
Female survival to 40 years
0.0
0.2
0.4
0.6
0.8
1.0
0.00
0.04
0.08
0.12
$F_{ROH,10Mb}$
B
Population Size
0
50
100
150
200
No inbreeding depression
Inbreeding depression
0
20
40
60
80
100
Year

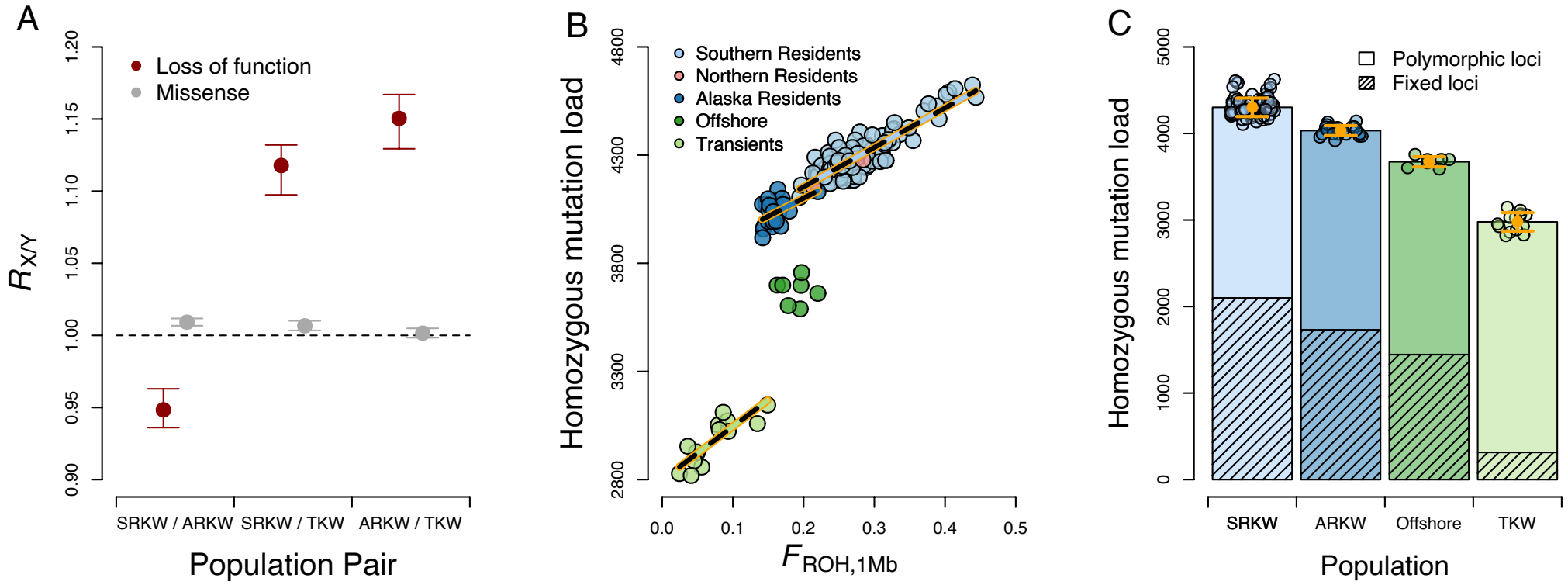
A
Loss of function
Missense
$R_{X/Y}$
0.90
0.95
1.00
1.05
1.10
1.15
1.20
SRKW / ARKW
SRKW / TKW
ARKW / TKW
Population Pair
B
Southern Residents
Northern Residents
Alaska Residents
Offshore
Transients
Homozygous mutation load
2800
3300
3800
4300
4800
0.0
0.1
0.2
0.3
0.4
0.5
$F_{ROH,1Mb}$
C
Polymorphic loci
Fixed loci
Homozygous mutation load
0
1000
2000
3000
4000
5000
SRKW
ARKW
Offshore
TKW
Population

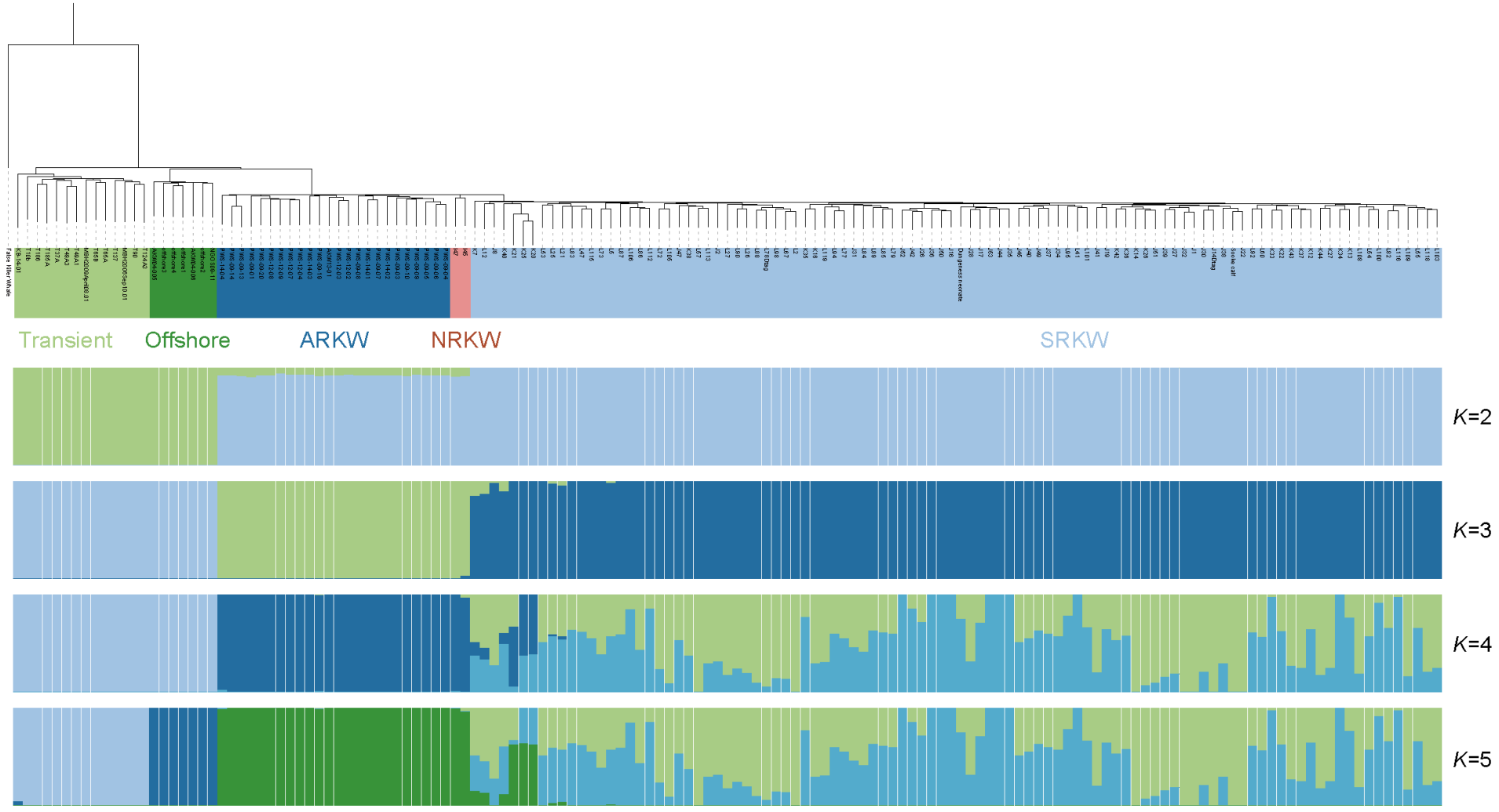
Transient
Offshore
ARKW
NRKW
SRKW
K=2
K=3
K=4
K=5

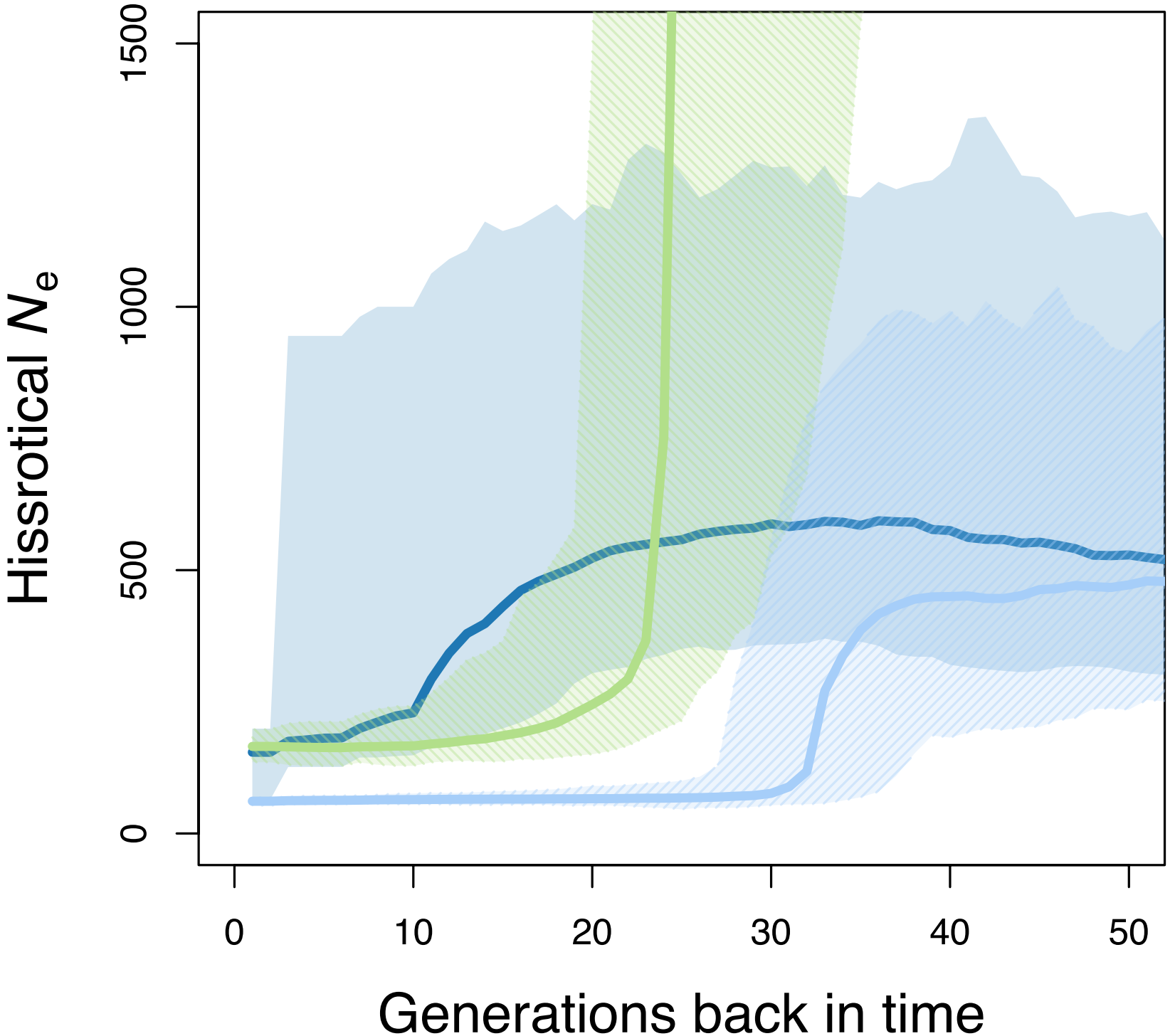
Hissrotical N_e
0
500
1000
1500
0
10
20
30
40
50
Generations back in time

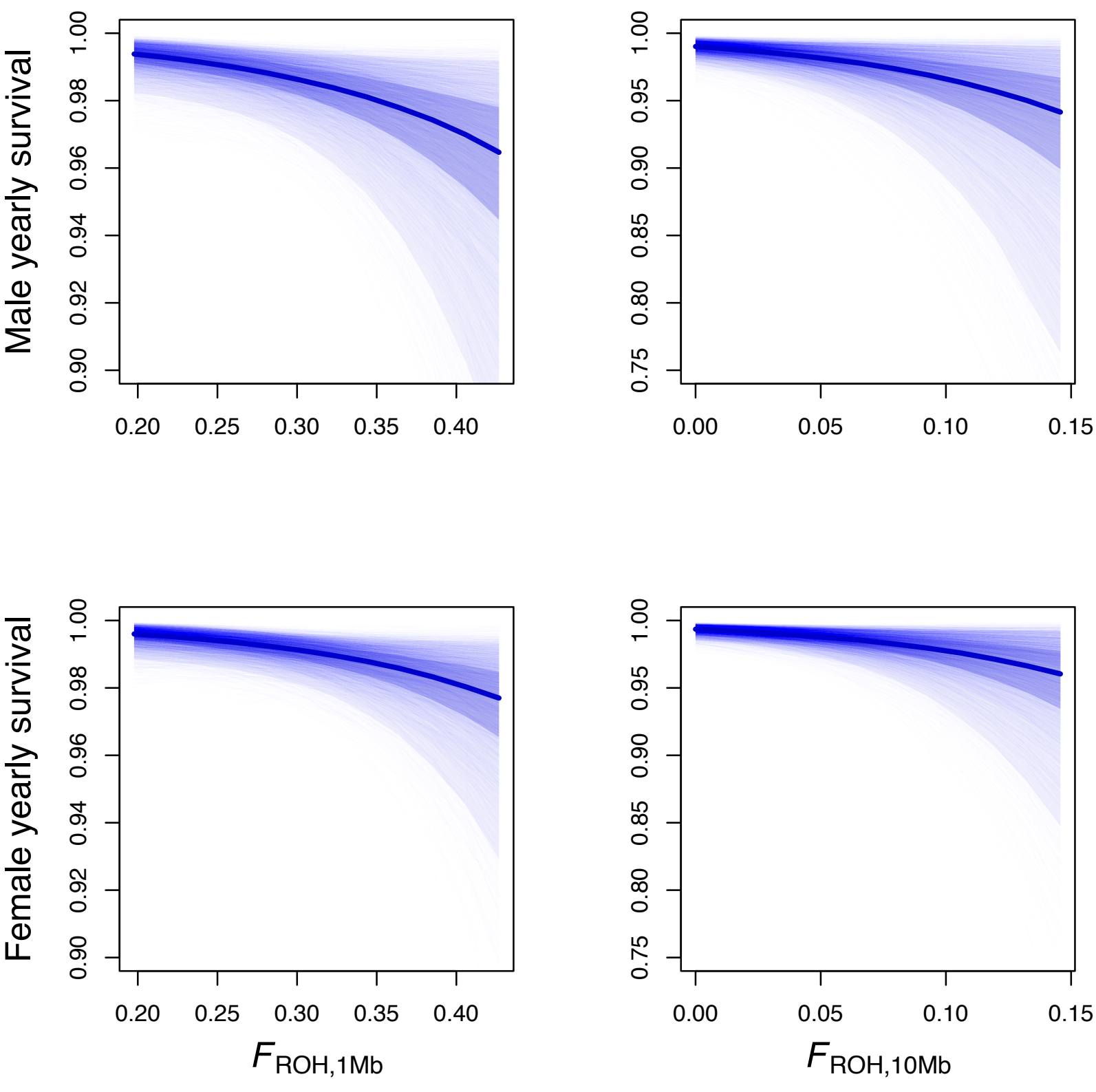
Male yearly survival
Female yearly survival
1.00
0.98
0.96
0.94
0.92
0.90
0.95
0.90
0.85
0.80
0.75
0.20
0.25
0.30
0.35
0.40
0.00
0.05
0.10
0.15
$F_{ROH,1Mb}$
$F_{ROH,10Mb}$

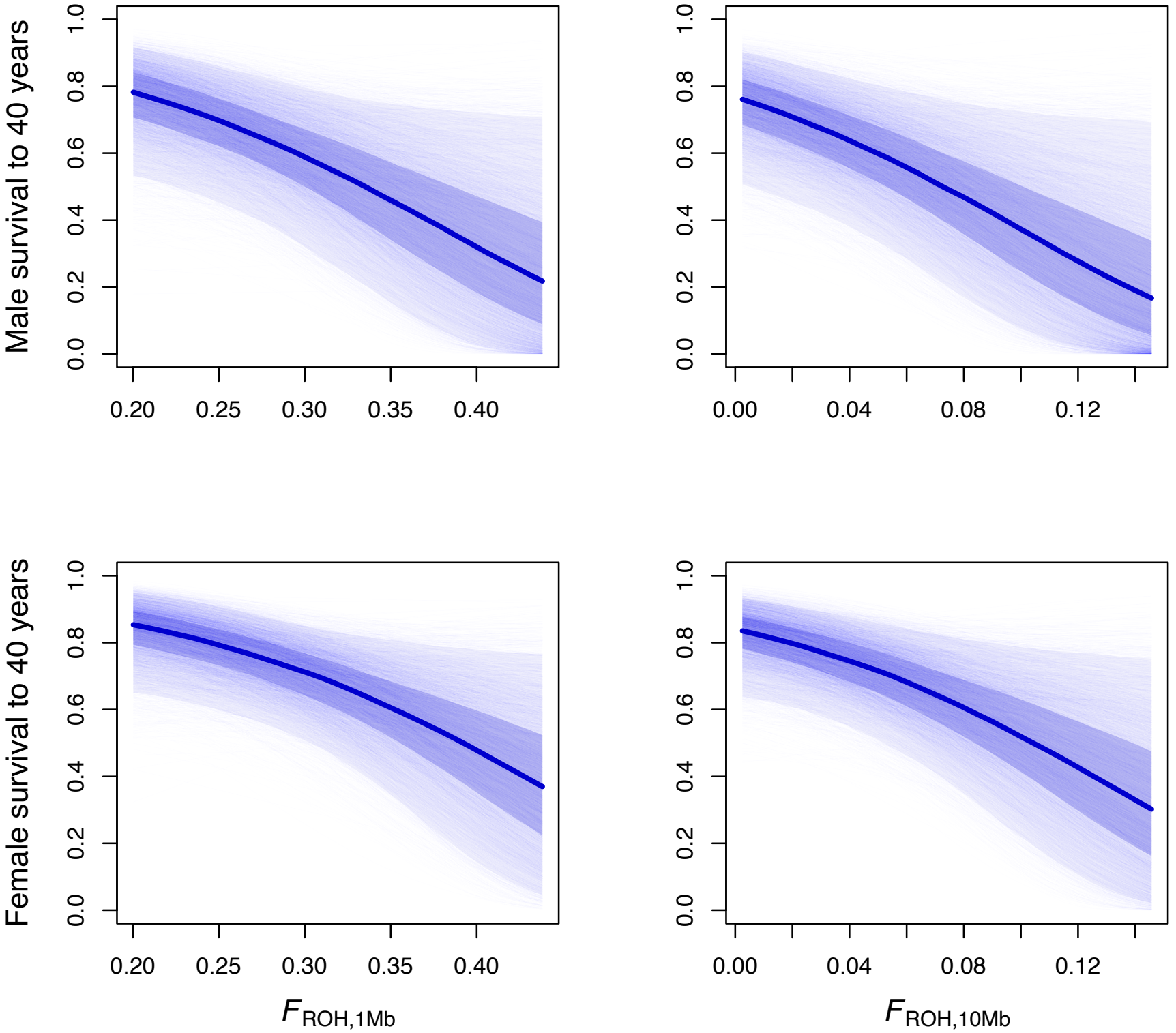
Male survival to 40 years
Female survival to 40 years
0.0
0.2
0.4
0.6
0.8
1.0
0.20
0.25
0.30
0.35
0.40
0.00
0.04
0.08
0.12
$F_{ROH,1Mb}$
$F_{ROH,10Mb}$

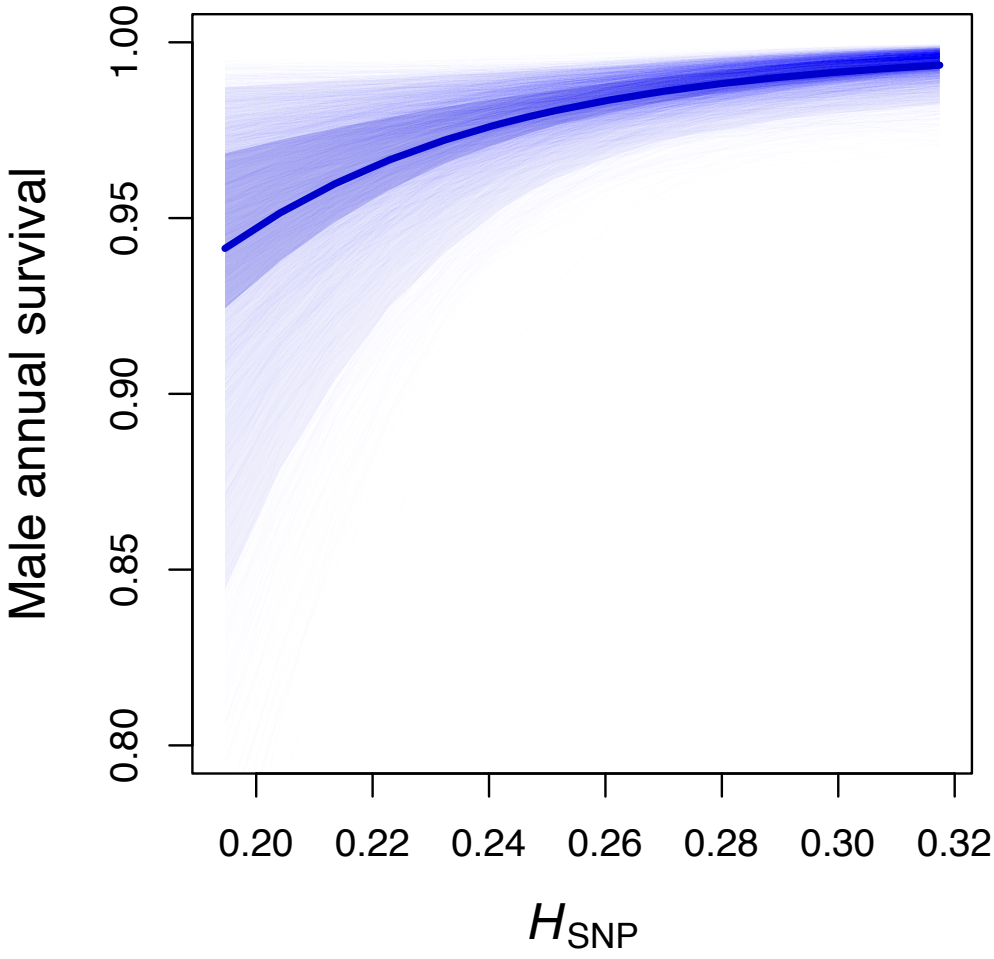
Male annual survival
1.00
0.95
0.90
0.85
0.80
0.20
0.22
0.24
0.26
0.28
0.30
0.32
H_{SNP}

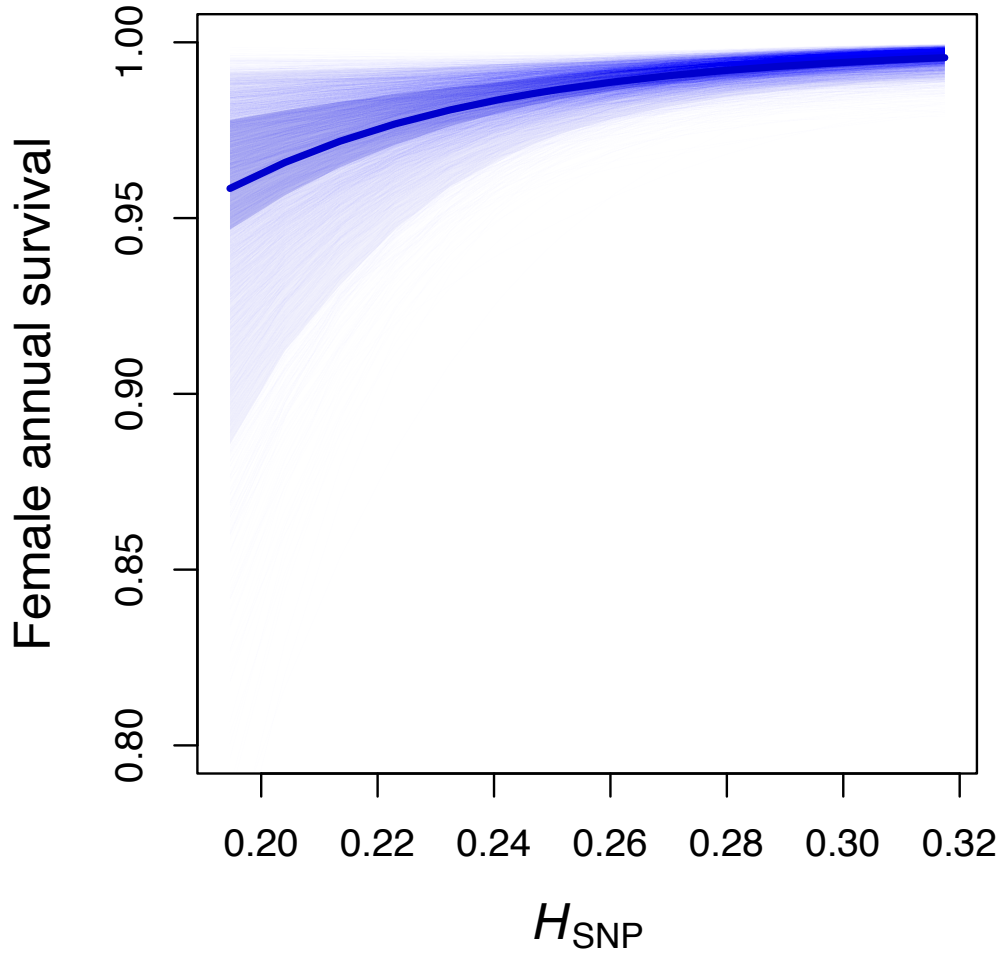
Female annual survival
1.00
0.95
0.90
0.85
0.80
0.20
0.22
0.24
0.26
0.28
0.30
0.32
H_{SNP}

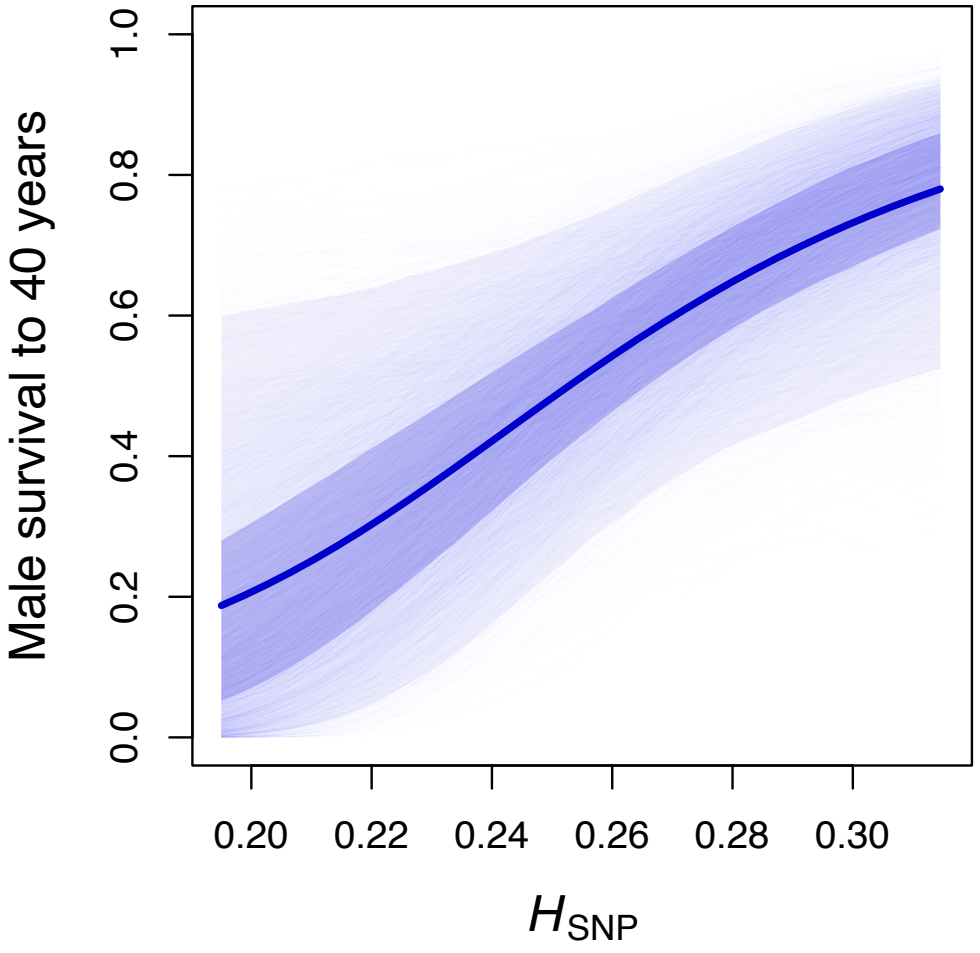
Male survival to 40 years
0.0
0.2
0.4
0.6
0.8
1.0
0.20
0.22
0.24
0.26
0.28
0.30
H_{SNP}

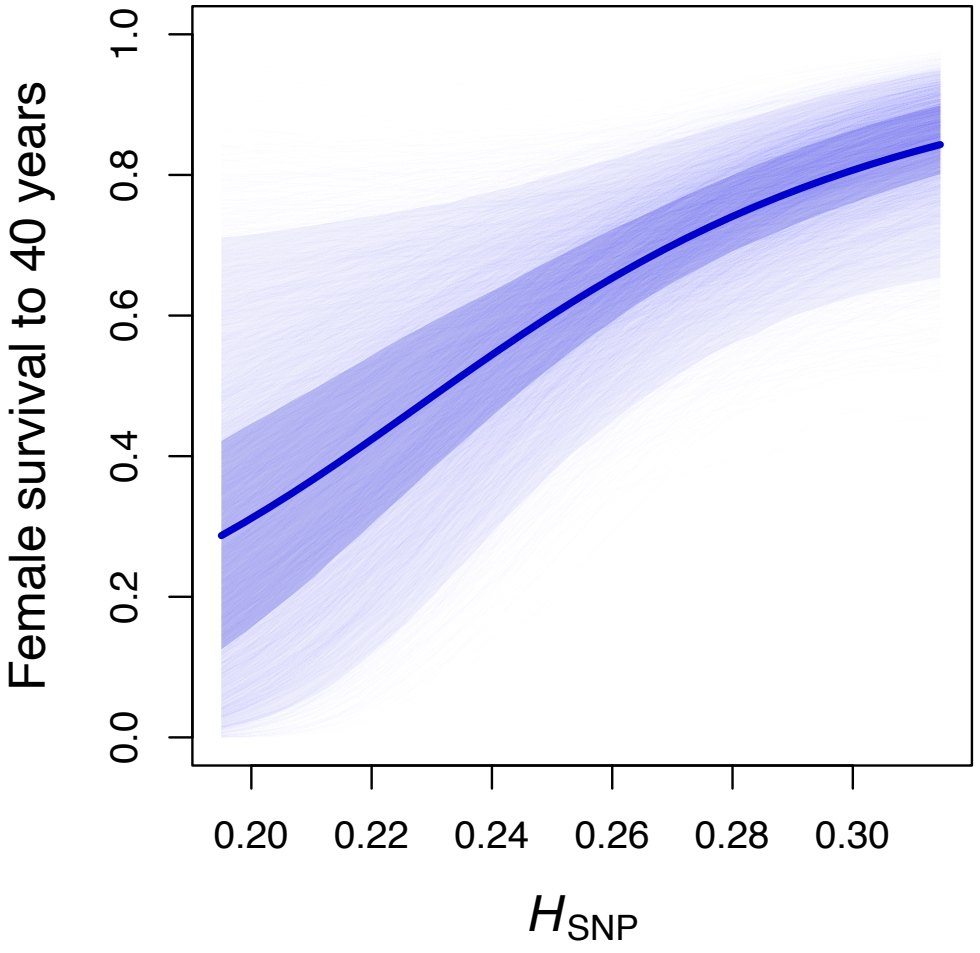
Female survival to 40 years
0.0
0.2
0.4
0.6
0.8
1.0
0.20
0.22
0.24
0.26
0.28
0.30
H_{SNP}

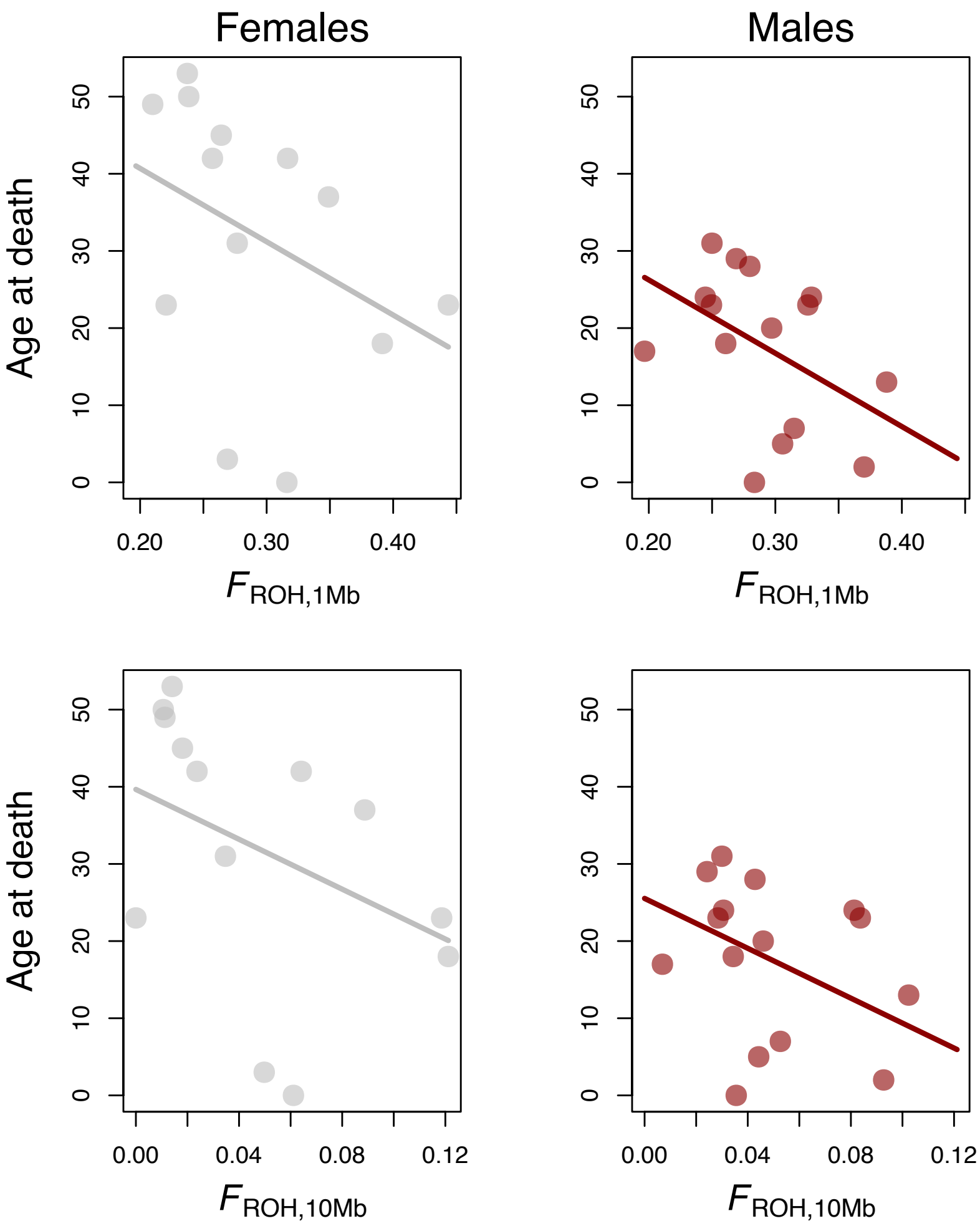
Females
Males
Age at death
0
10
20
30
40
50
0.20
0.30
0.40
$F_{ROH,1Mb}$
0.00
0.04
0.08
0.12
$F_{ROH,10Mb}$

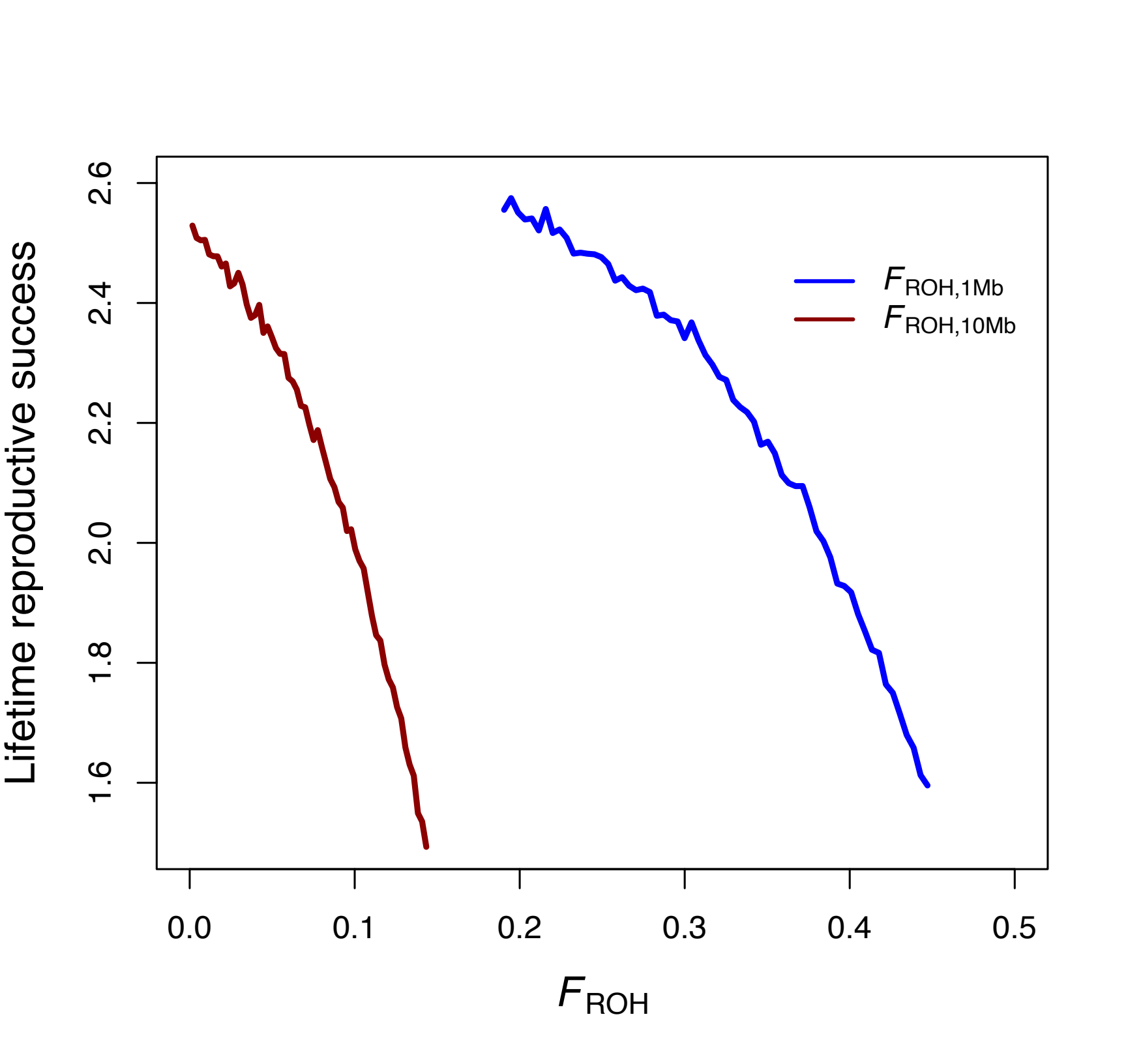
Lifetime reproductive success
1.6
1.8
2.0
2.2
2.4
2.6
0.0
0.1
0.2
0.3
0.4
0.5
F_{ROH}
$F_{ROH,1Mb}$
$F_{ROH,10Mb}$

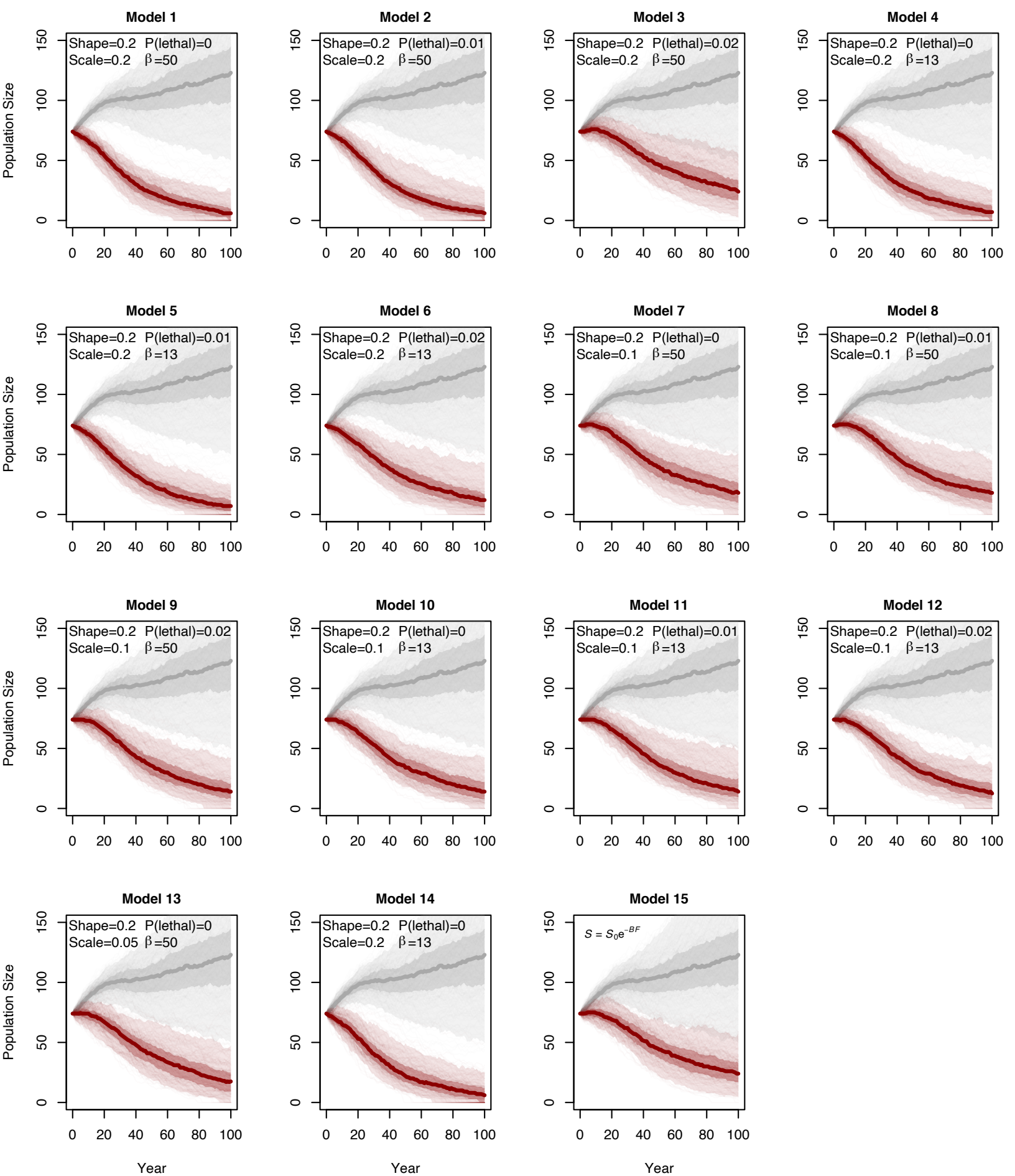
Model 1
Shape=0.2 P(lethal)=0
Scale=0.2 β=50
Model 2
Shape=0.2 P(lethal)=0.01
Scale=0.2 β=50
Model 3
Shape=0.2 P(lethal)=0.02
Scale=0.2 β=50
Model 4
Shape=0.2 P(lethal)=0
Scale=0.2 β=13
Model 5
Shape=0.2 P(lethal)=0.01
Scale=0.2 β=13
Model 6
Shape=0.2 P(lethal)=0.02
Scale=0.2 β=13
Model 7
Shape=0.2 P(lethal)=0
Scale=0.1 β=50
Model 8
Shape=0.2 P(lethal)=0.01
Scale=0.1 β=50
Model 9
Shape=0.2 P(lethal)=0.02
Scale=0.1 β=50
Model 10
Shape=0.2 P(lethal)=0
Scale=0.1 β=13
Model 11
Shape=0.2 P(lethal)=0.01
Scale=0.1 β=13
Model 12
Shape=0.2 P(lethal)=0.02
Scale=0.1 β=13
Model 13
Shape=0.2 P(lethal)=0
Scale=0.05 β=50
Model 14
Shape=0.2 P(lethal)=0
Scale=0.2 β=13
Model 15
$S = S_0 e^{-BF}$
Population Size
Year
0
50
100
150
0
20
40
60
80
100

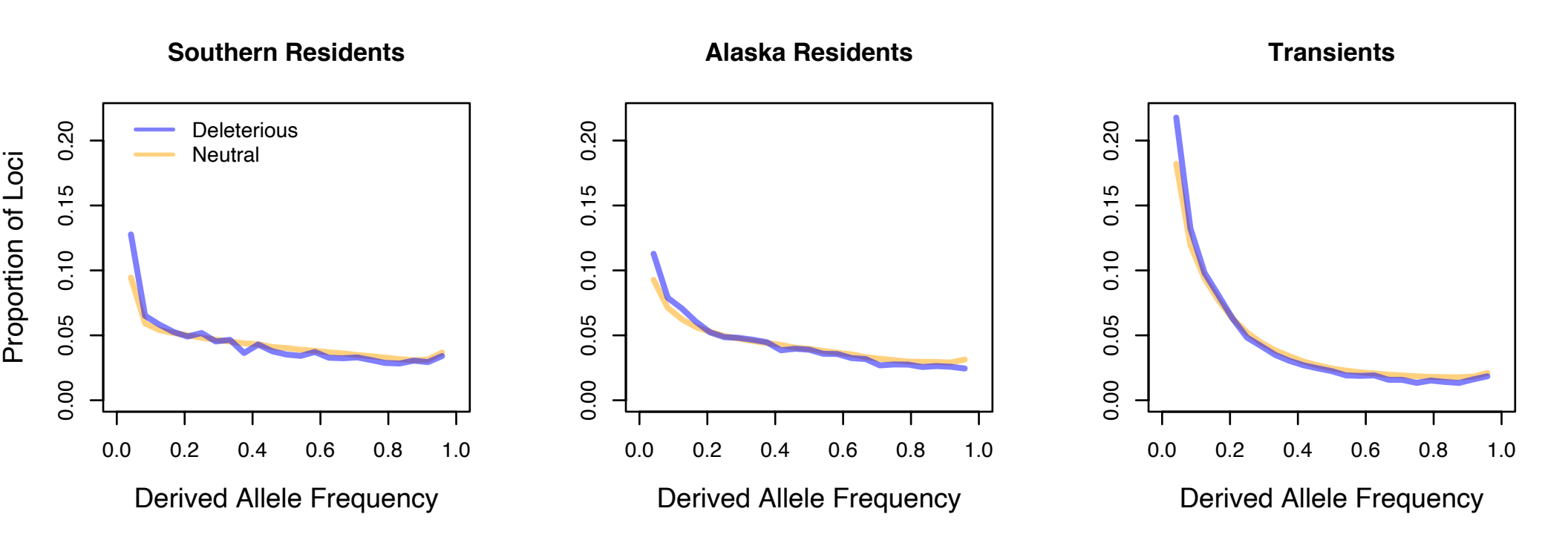
Southern Residents
Alaska Residents
Transients
Deleterious
Neutral
Proportion of Loci
0.00
0.05
0.10
0.15
0.20
0.0
0.2
0.4
0.6
0.8
1.0
Derived Allele Frequency